2. Abraham E, Arcaroli J, Carmody A, *et al.* Cutting edge: HMG-1 as a mediator of acute lung inflammation. J Immunol 2000;165:2950–2954.
3. Wang H, Yang H, Tracey KJ. Extracellular role of HMGB1 in inflammation and sepsis. J Intern Med 2004;255:320–331.
4. Ueno H, Matsuda T, Hashimoto S, *et al.* Contributions of high mobility group box protein in experimental and clinical acute lung injury. Am J Respir Crit Care Med 2004;170:1310–1316.
5. Wichterman KA, Baue AE, Chaudry IH. Sepsis and septic shock—a review of laboratory models and a proposal. J Surg Res 1980;29:189–201.
6. Baker CC, Chaudry IH, Gaines HO, *et al.* Evaluation of factors affecting mortality rate after sepsis in a murine cecal ligation and puncture model. Surgery 1983;94:331–335.
7. Anton EO, Quintela AG, Soto AL, *et al.* Cecal ligation and puncture as a model of sepsis in the rat: influence of the puncture size on mortality, bacteremia, endotoxemia and tumor necrosis factor alpha levels. Eur Surg Res 2001;33:77–79.
8. Heuer JG, Bailey DL, Sharma GR, *et al.* Cecal ligation and puncture with total parenteral nutrition: a clinically relevant model of the metabolic, hormonal, and inflammatory dysfunction associated with critical illness. J Surg Res 2004;121:178–186.
9. Andersson U, Tracey KJ. HMGB1 in sepsis. Scand J Infect Dis 2003;35:577–584.
10. Muller S, Ronfani L, Bianchi ME. Regulated expression and subcellular localization of HMGB1, a chromatin protein with a cytokine function. J Intern Med 2004;255:332–343.
11. Querini PR, Capobianco A, Scaffidi P, *et al.* HMGB1 is an endogenous immune adjuvant released by necrotic cells. EMBO Rep 2004;5:825–830.
12. Yang H, Ochani M, Li J, *et al.* Reversing established sepsis with antagonists of endogenous high-mobility group box 1. Proc Natl Acad Sci USA 2004;101:296–301.
13. Jensenius JC, Andersen I, Hau J, *et al.* Eggs: conveniently packaged antibodies. Methods for purification of yolk IgG. J Immunol Methods 1981;46:63–68.
14. Abeyama K, Stern DM, Ito Y, *et al.* The N-terminal domain of thrombomodulin sequesters high-mobility group-B1 protein, a novel anti-inflammatory mechanism. J Clin Invest 2005;115:1267–1274.
15. Yamada S, Inoue K, Yakabe K, *et al.* High mobility group protein 1 (HMGB1) quantified by ELISA with a monoclonal antibody that does not cross-react with HMGB2. Clin Chem 2003;49:1535–1537.
16. Naito Z, Ishiwata T, Kurban G, *et al.* Expression and accumulation of lumican protein in uterine cervical cancer cells at the periphery of cancer nests. Int J Oncol 2002;20:943–948.
17. Glyn E, Evans V, Sigurgeirsson B. Double blind, randomised study of continuous terbinafine compared with intermittent itraconazole in treatment of toenail onychomycosis. BMJ 1999;318:1031–1035.
18. Suda K, Kitagawa Y, Ozawa S, *et al.* Serum concentrations of high-mobility group box chromosomal protein 1 before and after exposure to the surgical stress of thoracic esophagectomy: a predictor of clinical course after surgery? Dis Esophagus 2006;19:5–9.
19. Ono S, Aosasa S, Mochizuki H. Effects of a protease inhibitor on reduction of surgical stress in esophagectomy. Am J Surg 1999;177:78–82.
20. Sato N, Koeda K, Ikeda K, *et al.* Randomized study of the benefits of preoperative corticosteroid administration on the postoperative morbidity and cytokine response in patients undergoing surgery for esophageal cancer. Ann Surg 2002;236:184–190.
21. Sato N, Endo S, Kimura Y, *et al.* Influence of a Human Protease inhibitor on surgical stress induced immunosuppression. Dig Surg 2002;19:300–305.
22. Watanabe T, Kubota S, Nagaya M, *et al.* The role of HMGB-1 on the development of necrosis during hepatic ischemia and hepatic ischemia/reperfusion injury in mice. J Surg Res 2005;124:59–66.
23. Czura CJ, Yang H, Tracey KJ. High mobility group box-1 as a therapeutic target downstream tumor necrosis factor. J Infect Dis 2003;187:S391–S396.
24. Mitchell BR, Ochani M, Li J, *et al.* IFN-γ induces high mobility group box 1 protein release partly through a TNF-dependent mechanism. J Immunol 2003;170:3890–3897.
25. Yang H, Wang H, Tracey KJ. HMG-1 rediscovered as a cytokine. Shock 2001;15:247–253.

BRCA1 Ubiquitinates RPB8 in Response to DNA Damage

Wenwen Wu,[1] Hiroyuki Nishikawa,[1] Ryosuke Hayami,[1] Ko Sato,[1] Akeri Honda,[1] Satoko Aratani,[2] Toshihiro Nakajima,[2] Mamoru Fukuda,[1] and Tomohiko Ohta[1]

[1]Division of Breast and Endocrine Surgery and [2]Department of Genome Science, Institute of Medical Science, St. Marianna University School of Medicine, Kawasaki, Japan

Abstract

The breast and ovarian tumor suppressor BRCA1 catalyzes untraditional polyubiquitin chains that could be a signal for processes other than proteolysis. However, despite intense investigations, the mechanisms regulated by the enzyme activity remain only partially understood. Here, we report that BRCA1-BARD1 mediates polyubiquitination of RPB8, a common subunit of RNA polymerases, in response to DNA damage. A proteomics screen identified RPB8 as a protein modified after epirubicin treatment in BRCA1-dependent manner. RPB8 interacted with BRCA1-BARD1 and was polyubiquitinated by BRCA1-BARD1 *in vivo* and *in vitro*. BRCA1-BARD1 did not destabilize RPB8 *in vivo* but rather caused an increase in the amount of soluble RPB8. Importantly, RPB8 was polyubiquitinated immediately after UV irradiation in a manner sensitive to BRCA1 knockdown by RNA interference. Substitution of five lysine residues of RPB8 with arginine residues abolished its ability to be ubiquitinated while preserving its polymerase activity. HeLa cell lines stably expressing this ubiquitin-resistant form of RPB8 exhibited UV hypersensitivity accompanied by up-regulated caspase activity. Our findings suggest that ubiquitination of a common subunit of RNA polymerases is a mechanism underlying BRCA1-dependent cell survival after DNA damage. [Cancer Res 2007;67(3):951–8]

Introduction

Germ line mutation of the cancer susceptibility gene *BRCA1* causes familial breast and ovarian cancer. BRCA1 acts as a hub protein that coordinates many cellular pathways to prevent tumor progression. Accordingly, down-regulation of this key protein by mechanisms other than *BRCA1* gene mutation causes sporadic breast cancer (1). All cells defective in BRCA1 show genomic instability as evidenced by hypersensitivity to DNA damage, the presence of chromosomal abnormalities, and the loss of heterozygosity at multiple loci. These results are likely to stem from the failure of BRCA1 to function in DNA damage repair, transcriptional regulation, apoptosis induction, intra-S or G_2-M checkpoint function, and regulation of centrosome duplication (2–4).

Involvement of BRCA1 in multiple cellular processes is logical given its enzymatic function as a ubiquitin ligase (E3). In this capacity, it has the potential to interact with numerous protein substrates and subsequently influence the biological response of a cell at many points. BRCA1 contains an NH_2-terminal RING finger domain, a common motif found in ubiquitin ligases. It acquires significant ubiquitin ligase activity when bound to another conformationally similar RING finger protein, BARD1, as a RING heterodimer (5–8). The most common polyubiquitin chain is linked through Lys^{48} of ubiquitin and serves as a signal for rapid degradation of substrates by the proteasome-dependent proteolysis pathway (9). However, BRCA1-BARD1 has the unique capacity to catalyze Lys^{6}-linked polyubiquitin chains, and the ubiquitination mediated by BRCA1-BARD1 could signal a process other than degradation (10–13). Deleterious missense mutations in the RING finger domain of BRCA1 found in familial breast cancer abolish the E3 ligase activity of BRCA1-BARD1 (6, 7, 14), indicating that the E3 ligase activity is important for role of BRCA1 as a tumor suppressor.

One of the most significant functional features of BRCA1 is that it is a component of the RNA polymerase II holoenzyme (15, 16). BRCA1 specifically interacts with a large fraction of hyperphosphorylated, processive polymerase II (IIO), in preference to the hypophosphorylated polymerase II (IIA) found at promoters (17). It has been proposed that BRCA1 binds polymerase IIO complexes as part of a genome scanning function for DNA damage (18). However, how BRCA1 affects the polymerase II complexes after DNA damage remains partially understood. In this study, we identify RPB8 (also called hRPB17 or *POLR2H*), a common subunit of all three types of RNA polymerases, as a substrate of BRCA1 E3 ligase and show that BRCA1 ubiquitinates RPB8 immediately after DNA damage. HeLa cell lines stably expressing a ubiquitin-resistant form of RPB8 exhibited UV hypersensitivity, a known phenotype of BRCA1 deficiency. These results indicate a significant role of ubiquitin ligase activity of BRCA1 for cell survival after DNA damage and provide a new aspect of a common subunit of RNA polymerases in DNA damage responses.

Materials and Methods

Two-dimensional difference gel electrophoresis. Methods for fluorescence two-dimensional difference gel electrophoresis (DIGE) and mass spectrometric analysis are reported in the Supplementary Data.

Plasmids. cDNA for full-length human RPB8 was amplified by PCR from a MCF10A cell cDNA library using Pfx polymerase (Stratagene, La Jolla, CA). Mammalian expression plasmids for BRCA1, BARD1, ubiquitin, and their mutants were previously described (7, 11). The point mutations to substitute the Lys residue(s) of RPB8 with Arg were produced by site-directed mutagenesis (Stratagene). All plasmids used were verified by DNA sequencing.

Cell cultures and transfections. T47D, HCC1937 breast carcinoma cells, HeLa cervical carcinoma cells, and 293T transformed human kidney cells were cultured in DMEM supplemented with 10% FCS and 1% antibiotic-antimycotic agent (Life Technologies, Inc., Grand Island, NY) in 5% CO_2 at 37°C. MCF10A normal human breast epithelial cells were grown in DMEM/Ham's F12 (1:1) medium supplemented with 2.5% FCS, 100 ng/mL cholera toxin, 20 ng/mL epidermal growth factor, 500 ng/mL hydrocortisone,

Note: Supplementary data for this article are available at Cancer Research Online (http://cancerres.aacrjournals.org/).

Requests for reprints: Tomohiko Ohta, Division of Breast and Endocrine Surgery, Department of Surgery, St. Marianna University School of Medicine, Kawasaki 216-8511, Japan. Phone: 81-44-977-8111; Fax: 81-44-976-5964; E-mail: to@marianna-u.ac.jp.

doi:10.1158/0008-5472.CAN-06-3187

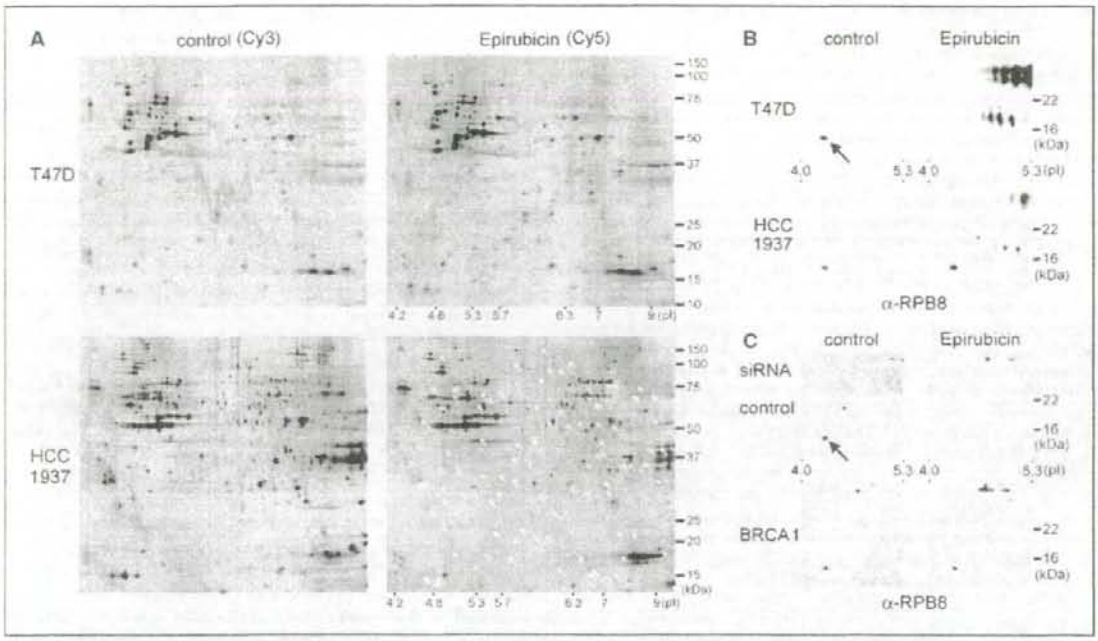

Figure 1. Proteomic screen for proteins affected by epirubicin treatment. *A*, T47D cells (*top*) and HCC1937 cells (*bottom*) were either untreated or treated with 0.2 μg/mL of epirubicin for 3 h and lysed with 7 mol/L urea/2 mol/L thiourea–containing buffer. Protein (50 μg) from untreated and epirubicin-treated cells was labeled with Cy3 (*left*) and Cy5 (*right*), respectively. The differently labeled samples were mixed together, resolved on a two-dimensional gel (pH range 3–10, *left* to *right*), and scanned with a fluorescence image analyzer. *Yellow arrows*, protein spots whose levels were significantly altered after epirubicin treatment. *Red arrows*, proteins that significantly decreased only in T47D cells after epirubicin treatment. The slower-migrating protein was identified as RPB8 and the faster one was myosin light chain. *B*, T47D cells or HCC1937 cells were treated as in *A* and lysed with 7 mol/L urea/2 mol/L thiourea–containing buffer. Lysates (500 μg) were resolved on a two-dimensional gel (pH range 3–10). A part of the gel was subjected to immunoblot with anti-RPB antibody. *Arrow*, RPB8. *C*, T47D cells were transfected either with control siRNA (*top*) or with siRNA for BRCA1 (*bottom*), treated with or without epirubicin, and subjected to anti-RPB8 immunoblotting as in *B*.

10 μg/mL insulin, and 1% antibiotic-antimycotic agent. For epirubicin treatment, cells were incubated in medium containing 0.2 μg/mL epirubicin (Pfizer, New York, NY). To examine the half-life of proteins *in vivo*, cells were incubated with 10 μg/mL cycloheximide (Wako, Osaka, Japan), a protein synthesis inhibitor, for the indicated time periods. 293T cells were transfected using the standard calcium phosphate precipitation method. To generate cell lines that stably expressed either wild-type (WT) or mutant FLAG-RPB8, HeLa cells were transfected using FuGENE6 (Roche, Indianapolis, IN) with pcDNA3 plasmids encoding each protein and selected with G418. For UV irradiation studies, cells were washed with PBS, irradiated with UV light (254 nm; UVP, Inc., Upland, CA) at the indicated doses, and grown in fresh medium for various times.

Antibodies. Mouse monoclonal antibodies to hemagglutinin (HA; Boehringer-Mannheim, Mannheim, Germany), Myc (BabCo, Richmond, CA), FLAG (Sigma, St. Louis, MO), polyubiquitin (Affiniti, Exeter, United Kingdom), conjugated ubiquitin (Affiniti; ref. 10), α- and β-tubulin (Neomarkers, Fremont, CA), and actin (Santa Cruz Biotechnology, Santa Cruz, CA) as well as rabbit polyclonal antibodies to BRCA1 (Santa Cruz Biotechnology), RPB1 (Covance), and cleaved caspase-3 (Cell Signaling Technology, Danvers, MA) were purchased commercially. Anti-FLAG cross-linked agarose beads (Sigma) were used for immunoprecipitation to detect *in vivo* ubiquitinated substrates. Rabbit polyclonal antibodies to BARD1 and RPC155 were generous gifts from Dr. Richard Baer (Columbia University, New York, NY) and Dr. Nouria Hernandez (Cold Spring Harbor Laboratory, Cold Spring Harbor, NY), respectively. Rabbit polyclonal antibody to RPB8 was generated against full-length human glutathione *S*-transferase (GST)-RPB8 and purified by protein G agarose chromatography.

RNA interference. SMART pool BRCA1 small interfering RNA (siRNA) mix and control siRNA mix were purchased from Dharmacon Research, Inc. (Lafayette, CO). RNA duplexes (final concentration 50 nmol/L) were transfected into the cells with Oligofectamine (Invitrogen, Carlsbad, CA) according to the manufacturer's instructions. Retrovirus expressing short hairpin RNA (shRNA) that targets BRCA1 mRNA sequence 5′-CUAGAAAU-CUGUUGCUAUG-3′ was created by cotransfecting 293T cells with pGP vector, pE-ampho vector, and pSINsi-hU6 retroviral vector that has previously been subcloned with the oligonucleotide 5′-GATCCGCTA-GAAATCTGTTGCTATGTTCAAGAGACATAGCAACAGATTTCTAGCTTTTT-TAT-3′ according to the manufacturer's protocol (TaKaRa, Otsu, Japan). Oligonucleotide 5′-GATCCGTAAGGCTATGAAGAGATACTTCAAGAGAG-TATCTCTTCATAGCCTTACTTTTTTAT-3′ was used for the retrovirus expressing control shRNA. For infection, HeLa cells were incubated with virus supernatants and fresh culture medium containing 8 μg/mL Polybrene (Sigma). Cells were analyzed 48 h after transfection or infection.

Immunoprecipitation and immunoblotting. Immunoprecipitation and immunoblotting methods were previously described (11). For the immunoblotting analysis after two-dimensional gel electrophoresis, cells were lysed with 7 mol/L urea/2 mol/L thiourea–containing buffer as described above. Soluble fractions were prepared with 0.5% NP40-based buffer as previously described (11). Denatured whole-cell lysates were prepared by boiling in Laemmli SDS-loading buffer with 0.1 mol/L DTT.

***In vitro* ubiquitin ligation assay.** Full-length His-FLAG-RPB8 was obtained from BL21/DE3 bacteria cells with isopropyl-L-thio-β-D-galacto-pyranoside induction by two-step purification using nickel agarose beads followed by anti-FLAG cross-linked agarose beads (Supplementary Fig. S3). Complexes of WT or I26A mutant of FLAG-BRCA1$^{1-772}$ with BARD1 were

purified from transfected 293T cells by anti-FLAG affinity chromatography and FLAG peptide elution. Both WT and I26A mutant complexes contained an ~1:1 ratio of BRCA1 and BARD1 proteins (Supplementary Fig. S3). Rabbit E1 (BIOMOL, Plymouth Meeting, PA) and mammalian ubiquitin (Boston Biochem, Cambridge, MA) were purchased commercially. The *in vitro* reaction was done as previously described (11) with a reaction mixture (30 μL) that contained 0.5 μg His-FLAG-RPB8, 40 ng E1, 0.3 μg UbcH5c, and 0.3 μg each of FLAG-BRCA1$^{1-772}$ and BARD1.

Runoff transcription assay. The runoff transcription assay used was described elsewhere (17). Briefly, the runoff template was created by annealing 50 pmol each of a 65-mer oligonucleotide 5′-ATTGGGTAAAGGAGAGTATTTGAGCGGAGGACAGTACTCCGGGTCCCCCCCCCCCCCCCCCCCC-3′and a complementary 45-mer oligonucleotide 5′-GACCCGGAGTACTGTCCTCCGCTCTTTTACTCTCCTTTACCCAAT-3′ in a 200 μL annealing mixture containing 20 mmol/L Tris (pH 7.4), 1 mmol/L EDTA, and 0.2 mol/L NaCl. Runoff transcription reactions (20 μL) contained 8.25 mmol/L $MgCl_2$, 5 μg of bovine serum albumin, 250 nmol/L nucleotide triphosphates, 5 units of RNase inhibitor, 50 ng of poly(deoxyinosinic-deoxycytidylic acid), 0.05% NP40, 1 pmol of annealed oligonucleotides, and 0.5 μCi of [α-^{32}P]CTP. Equilibrated FLAG-RPB8 immunocomplexes bound to M2 beads (10 μL) were added to the reactions (20 μL) and incubated for 40 min at 30°C and stopped with 50 μL of PK buffer (300 mmol/L sodium acetate, 0.2% SDS, 10 mmol/L EDTA, 100 ng tRNA, and 10 μg proteinase K). Reactions were then incubated at 55°C for 20 min, extracted with phenol/chloroform, and precipitated with ethanol. Single-stranded RNA transcripts were resolved under denaturing conditions on 12% polyacrylamide/urea gels and scanned with the Typhoon 9400 image analyzer (Amersham, Piscataway, NJ).

Results

Identification of RPB8 as a protein modified in BRCA1-positive cells after epirubicin treatment. To search for candidate substrates for the BRCA1-BARD1 E3 ligase in response to DNA damage, we used two-dimensional DIGE technology. Breast cancer–derived, BRCA1–positive T47D cells and BRCA1-defective HCC1937 cells were incubated for 3 h with epirubicin, a topoisomerase II inhibitor that induces DNA double strand breaks. Cells were lysed with 7 mol/L urea/2 mol/L thiourea–containing buffer, and the proteomes were compared with untreated cells using two-dimensional DIGE. Interestingly, whereas the expression levels of only a few proteins were affected by the epirubicin treatment in T47D cells, that of ~100 proteins were altered in HCC1937 cells (Fig. 1*A*). Conversely and even more interesting, two proteins whose expression levels were dramatically reduced in T47D cells were not changed in HCC1937 cells (Fig. 1*A*, *red arrows*). Therefore, we speculated that the reduction could depend on the presence of BRCA1. The protein spots were in-gel digested and subjected to nanoscale capillary liquid chromatography-tandem mass spectrometry (LC/MS/MS) analysis. LC/MS/MS analysis revealed that the samples were RPB8, a common subunit of three types of RNA polymerases, and myosin light chain. RPB8 is a very acidic, small protein with a calculated molecular mass of 17.1 kDa and an isoelectric point of 4.34 (19). One of the most significant functional features of BRCA1 is that it is a component of the RNA polymerase II holoenzyme (15, 16). Therefore, we focused on RPB8 for further analyses.

To confirm our mass spectrometry data, we generated a rabbit polyclonal antibody to GST-RPB8 for immunoblot analysis. Cells were treated as in Fig. 1*A*, and immunoblot analysis of the proteins resolved by two-dimensional gels verified that the protein spot was indeed RPB8. It was again severely reduced by epirubicin treatment only in T47D cells (Fig. 1*B*). The difference in RPB8 expression in response to epirubicin treatment could be due to the different genetic backgrounds of these two cell lines, not just the absence or presence of BRCA1. Therefore, we next compared RPB8 expression between isogenic cells with and without knockdown of BRCA1

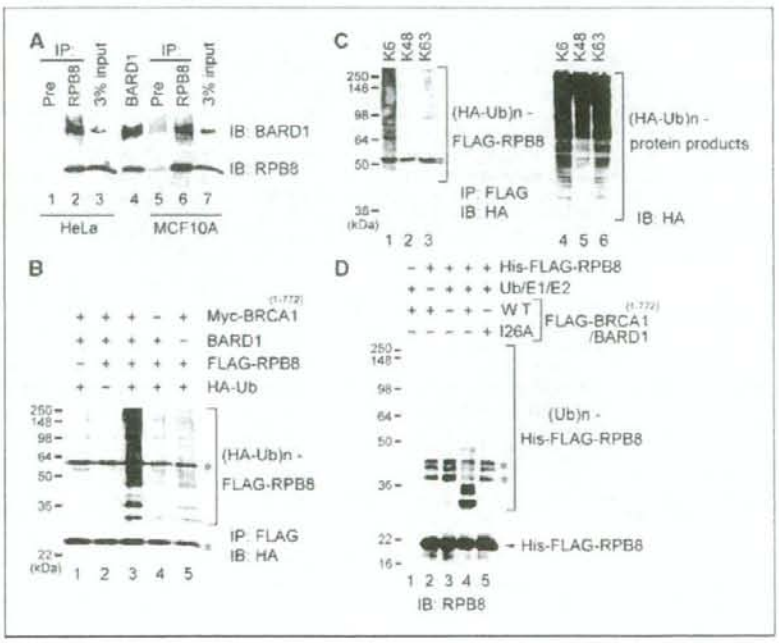

Figure 2. RPB8 and BARD1 interaction, and RPB8 ubiquitination by BRCA1-BARD1. *A*, endogenous RPB8 interacts with BARD1. Lysates prepared from HeLa (*lanes 1–3*) or MCF10A (*lanes 5–7*) cells were immunoprecipitated (*IP*) with anti-RPB8 or preimmune serum (*Pre*) and analyzed by immunoblotting (*IB*) using the indicated antibodies. A portion of the cell lysates corresponding to 3% of the input for immunoprecipitation as well as lysate from 293T cells transfected with BARD1 (*lane 4*) were also loaded. *B*, 293T cells transfected with the indicated plasmids were boiled in 1% SDS lysis buffer, diluted to 0.1% SDS, and immunoprecipitated with anti-FLAG antibody–cross-linked beads. Precipitated FLAG-RPB8 was resolved by 12.5% SDS-PAGE followed by immunoblotting with anti-HA antibody. *, IgG. *C*, polyubiquitination of RPB8 was detected as in *A*, except that HA-ubiquitin (*HA-Ub*) with a single lysine residue was transfected as indicated (*lanes 1–3*). A portion of the cell lysate was subjected to immunoblotting with anti-HA antibody to detect total HA-ubiquitin–conjugated proteins in cells as a control for protein expression (*lanes 4–6*). *, IgG. *D*, bacterially purified His-FLAG-RPB8 was incubated in the presence of ATP with ubiquitin, E1, E2/UbcH5c, and either WT or I26A mutant of FLAG-BRCA1$^{1-772}$/BARD1 complex as indicated and immunoblotted with anti-RPB8 antibody. *, nonspecific products copurified with His-FLAG-RPB8.

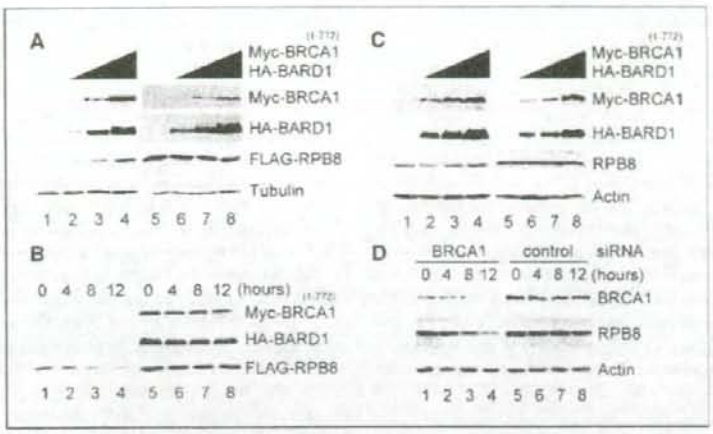

Figure 3. BRCA1-BARD1 did not destabilize RPB8 *in vivo* but rather caused an increase of RPB8 in the soluble fraction. *A*, 293T cells were transfected with plasmids encoding FLAG-RPB8 (*lanes 1–8*, 0.3 μg) and increasing amounts of Myc-BRCA1$^{1-772}$ and HA-BARD1 (*lanes 2* and *6*, 2 μg; *lanes 3* and *7*, 4 μg; *lanes 4* and *8*, 7.35 μg each). Total plasmid DNA was adjusted to 15 μg per plate by adding the parental pcDNA3 vector. The steady-state level of each protein in the soluble fraction (*lanes 1–4*) and whole-cell lysates (*lanes 5–8*) was analyzed by immunoblot using anti-Myc, anti-HA, anti-FLAG, or anti-tubulin antibodies. *B*, 293T cells were transfected with plasmids encoding FLAG-RPB8 (0.2 μg, *lanes 1–4*) or Myc-BRCA1$^{1-772}$ and HA-BARD1 (1 μg each, *lanes 5–8*). Thirty-six hours after transfection, cells were incubated with cycloheximide (10 μmol/L) and chased for the indicated lengths of time. Soluble fractions of the cell lysates were then immunoblotted with Myc, HA, or FLAG antibody. *C*, steady-state levels of RPB8 were analyzed as in *A*, except that FLAG-RPB8 was not transfected and anti-RPB8 antibody was used to detect endogenous RPB8. *D*, T47D cells were transfected either with siRNA for BRCA1 (*lanes 1–4*) or control siRNA (*lanes 5–8*). Cells were incubated with cycloheximide (10 μmol/L) and chased for the indicated lengths of time. The soluble fraction of the cell lysates was then immunoblotted with the indicated antibodies.

expression. T47D cells were transfected with either control siRNA or BRCA1 siRNA and then treated as in Fig. 1*A*. The siRNA-transfected cells were successfully silenced for BRCA1 expression (Supplementary Fig. S1). Immunoblot analysis of the proteins resolved by two-dimensional gels showed that RPB8 was reduced by epirubicin treatment only in control cells, not in cells with BRCA1 knockdown, supporting the idea that this modification depends on BRCA1 expression (Fig. 1*C*). The reduction of RPB8 at its normal migrating position could be due to protein degradation or to covalent modification.

BRCA1-BARD1 interacts with and ubiquitinates RPB8. The polymerase II holoenzyme interacts with BRCA1 and BARD1 (15, 16). Consistent with the previous reports, a significant amount of endogenous BARD1 coimmunoprecipitated with RPB8 isolated from HeLa cells or MCF10A cells compared with controls (Fig. 2*A*). The same results were observed with MCF7, T47D, and 293T cells (data not shown). Exogenously expressed RPB8 also interacted with BRCA1 and BARD1 (Supplementary Fig. S2). Then, we tested whether RPB8 is ubiquitinated by BRCA1-BARD1 *in vivo*. FLAG-RPB8 was coexpressed in 293T cells with HA-ubiquitin, Myc-BRCA1$^{1-772}$, and BARD1. Cells were collected 36 h after transfection and boiled in 1% SDS–containing buffer, and FLAG-RPB8 was immunoprecipitated. Immunoblotting of the RPB8 precipitates resolved by SDS-PAGE using anti-HA antibody showed a ladder characteristic of polyubiquitinated RPB8 (Fig. 2*B*). Omission of FLAG-RPB8, HA-ubiquitin, Myc-BRCA1$^{1-772}$, or BARD1 all abolished the RPB8 ladders, supporting the idea of BRCA1-BARD1–dependent RPB8 ubiquitination.

BRCA1-BARD1 is the only known E3 ligase to catalyze Lys^{6}-linked polyubiquitin chains (10, 11, 13). To show that the *in vivo* RPB8 ubiquitin ladders were directly due to BRCA1-BARD1 ligase activity, we verified that RPB8 was modified by ubiquitin through Lys^{6} linkages. HA-tagged ubiquitins that have a single lysine residue available for conjugation were used for *in vivo* ubiquitination assays. As expected, BRCA1-BARD1–dependent RPB8 polyubiquitination was predominantly detected when HA-ubiquitin with only Lys^{6} available, but not Lys^{48} or Lys^{63}, was coexpressed (Fig. 2*C*). However, it has been suggested that ubiquitin mutants could fold incorrectly and may cause artifacts (20). Recent quantitative analysis of *in vitro* ubiquitination revealed that even for cyclin B1 ubiquitination catalyzed by the anaphase-promoting complex, heterogeneous ubiquitin chains, including Lys^{63}, Lys^{11}, and Lys^{48}, or monoubiquitin attached to multiple lysine residues on the substrate. Further, some types of linkages are dependent on the combination of E2 and E3 enzymes (21). Thus, it is possible that ubiquitination mediated by BRCA1-BARD1 also resulted in multiple polyubiquitin chains, including Lys^{6}. The preference for Lys^{6} ubiquitination observed in the *in vivo* experiment was not enough evidence to support the direct role of BRCA1-BARD1 for RPB8 ubiquitination. Therefore, we further tested whether BRCA1-BARD1 directly catalyzes RPB8 polyubiquitination by *in vitro* ubiquitination using recombinant RPB8 protein (Supplementary Fig. S3). His-FLAG-RPB8 incubated with ubiquitin, E1, E2/His-UbcH5c, and FLAG-BRCA1$^{1-772}$/BARD1 complex (Supplementary Fig. S3) resulted in a ladder and smear detected by anti-RPB8 immunoblot (Fig. 2*D*). Omission of substrate RPB8, ubiquitin/E1/E2, or FLAG-BRCA1$^{1-772}$/BARD1 complex, as well as substitution of BRCA1$^{1-772}$ with the E2-nonbinding mutant I26A, all abolished RPB8 ubiquitination. Hence, the results suggest that the RPB8 polyubiquitination is directly catalyzed by BRCA1-BARD1.

BRCA1-BARD1 does not destabilize RPB8 *in vivo*. Our previous results suggested that BRCA1-BARD1 catalyzed untraditional polyubiquitin chains that served as a signal for a process other than degradation (7, 11, 12). However, the reduced expression of RPB8 after epirubicin treatment detected by two-dimensional DIGE or two-dimensional immunoblot (Fig. 1) suggested the

possibility of BRCA1-mediated RPB8 degradation. Therefore, we tested if BRCA1-BARD1 destabilized RPB8 *in vivo* under several different conditions, including BRCA1-BARD1 overexpression and BRCA1 knockdown by siRNA. FLAG-RPB8 was coexpressed in 293T cells with Myc-BRCA1$^{1-772}$ and HA-BARD1 (Fig. 3*A*). The steady-state level of FLAG-RPB8 increased upon coexpression of BRCA1-BARD1 in a dose-dependent manner in the soluble fraction (*lanes 1–4*) but not in whole-cell lysates (*lanes 5–8*). We then examined protein half-life of FLAG-RPB8 in the soluble fraction using cycloheximide, a protein synthesis inhibitor. The FLAG-RPB8 protein half-life was prolonged by BRCA1-BARD1 overexpression (Fig. 3*B*). We also tested the effect of BRCA1-BARD1 on endogenous RPB8 (Fig. 3*C* and *D*). The steady-state level of RPB8 only slightly increased upon coexpression of BRCA1-BARD1 in the soluble fraction (Fig. 3*C*, *lane 4*) and no effect was observed when whole-cell lysates were evaluated (*lanes 5–8*). However, RPB8 protein half-life was detectably shortened by BRCA1 knockdown (Fig. 3*D*). This observation was not detected when whole-cell lysates were analyzed (data not shown). Together, analyses of steady-state levels and protein half-lives indicated that only soluble RPB8 was stabilized, whereas that in whole-cell lysate was unchanged (Fig. 3). Alternatively, it was also possible that BRCA1-BARD1 shifted RPB8 from the insoluble fraction, such as the chromatin fraction, to the soluble fraction. However, we could not detect such a shift by fractionation analyses (data not shown). In either case, these findings at least suggest that BRCA1-BARD1–mediated RPB8 ubiquitination is not a signal for its degradation.

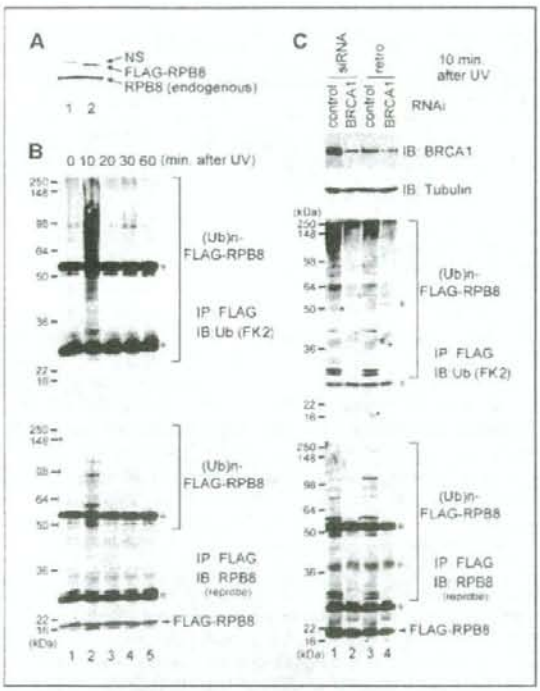

Figure 4. BRCA1-dependent RPB8 polyubiquitination in response to UV irradiation. *A*, parental HeLa cells (*lane 1*) and HeLa cells stably expressing FLAG-RPB8 (*lane 2*) were lysed with SDS-sample buffer and immunoblotted with anti-RPB8 antibody. *NS*, nonspecific products. *B*, HeLa cells stably expressing FLAG-RPB8 were UV irradiated (35 J/m^2) and harvested at the indicated times after irradiation. Ubiquitinated RPB8 was detected as described in Fig. 2*B*, except that anti-ubiquitin antibody (FK2) was used for immunoblotting (*top*). The membrane was reprobed with anti-RPB8 antibody (*bottom*). *C*, HeLa cells stably expressing FLAG-RPB8 were either transfected with control siRNA (*lane 1*), transfected with siRNA for BRCA1 (*lane 2*), infected with retrovirus expressing control shRNA (*lane 3*), or infected with retrovirus expressing shRNA for BRCA1 (*lane 4*). Cells were then UV irradiated (35 J/m^2) and harvested 10 min after irradiation. Cells were boiled in 1% SDS buffer and subjected either to immunoblotting with anti-BRCA1 (*top*) and antitubulin (*upper middle*) or to detection of RPB8 ubiquitination as in *B* (*lower middle* and *bottom*). *, IgG. Note that the different pattern of IgG detection between *B* and *C* is due to different lots of anti-FLAG cross-linked agarose beads.

BRCA1-dependent RPB8 ubiquitination after UV irradiation. BRCA1-mediated RPB8 ubiquitination prompted us to investigate the biological implications of this activity. We examined if RPB8 is ubiquitinated in response to DNA damage. Rather than exposing cells continuously to epirubicin, and because RPB1 is ubiquitinated after UV irradiation, we used UV irradiation to accurately determine the timing of RPB8 ubiquitination after DNA damage (22–25). We established HeLa cell lines that stably express FLAG-RPB8 at a low level (approximately one third of endogenous RPB8; Fig. 4*A*) to avoid artifacts caused by overexpression and analyzed ubiquitination of anti-FLAG immunoprecipitates with anti-ubiquitin (FK2) antibody. Because it has been reported that RPB1 ubiquitination occurs 1 to 2 h after UV irradiation (22–25), we first analyzed these time points. However, we did not detect any ubiquitination of FLAG-RPB8 (Fig. 4*B* and data not shown). Instead, ubiquitinated FLAG-RPB8 readily, and only transiently, appeared 10 min after UV irradiation (Fig. 4*B*, *top*). Reprobing the membrane with anti-RPB8 antibody verified that the detected ladder was ubiquitinated RPB8 (*bottom*).

To verify that UV irradiation–induced RPB8 ubiquitination requires endogenous BRCA1, RNA interference was used to knock down BRCA1 expression. HeLa cells stably expressing FLAG-RPB8 were transfected with BRCA1-specific siRNA. As a second alternative, we constructed a retrovirus engineered to express shRNA for BRCA1. Forty-eight hours after transfection or infection, cells were irradiated with UV (35 J/m^2) and then harvested 10 min later. Both the siRNA-transfected and the shRNA retrovirus–infected cells were successfully silenced for BRCA1 expression (>90% and >75% reduction, respectively) compared with their controls (Fig. 4*C*, *top*). As expected, RPB8 ubiquitination after UV irradiation was dramatically reduced by BRCA1 knockdown in both cases (*lower middle*). Reprobing the membrane with anti-RPB8 antibody again verified the ubiquitinated RPB8 that became completely undetectable upon BRCA1 knockdown (*bottom*). These results support the idea that RPB8 is polyubiquitinated by BRCA1-BARD1 in an early phase after UV irradiation.

A ubiquitin-resistant form of RPB8 retains its polymerase activity. For the purpose of studying the physiologic consequences induced by the BRCA1-mediated RPB8 ubiquitination after UV irradiation, we generated a mutant of RPB8 that is incapable of being ubiquitinated by BRCA1-BARD1. RPB8 possesses eight Lys residues in the whole protein (Fig. 5*A*). We first mutated single Lys residues of RPB8 and tested its capacity to be ubiquitinated. However, RPB8 ubiquitination was not dramatically reduced by each single mutation (Fig. 5*B*, *lanes 2* and *7*; data not shown). Instead, the ubiquitination of RPB8 was reduced as the number of Lys to Arg substitutions increased. This result recapitulates what we observed during studies of BRCA1 auto-ubiquitination and of BRCA1-mediated NPM1/B23 ubiquitination. When five of the eight Lys residues were substituted with Arg (5KR), RPB8 ubiquitination

became undetectable (Fig. 5*B*, *lane 5*), although its binding capacity to BRCA1-BARD1 was not reduced (data not shown).

To confirm that the many mutations required to make RPB8 resistant to ubiquitination did not impair its fundamental function as a subunit of RNA polymerases, we verified that the 5KR mutant is capable of binding to RPB1 or RPC155 (the largest subunit of polymerase III) *in vivo*. WT FLAG-RPB8 or 5KR was transfected into 293T cells, and anti-FLAG immunocomplexes were isolated. Bound proteins were resolved by SDS-PAGE and analyzed by immunoblotting using anti-RPB1 or anti-RPC155 antibodies. Both RPB1 and RPC155 were detected in the FLAG-5KR immunocomplexes as well as the WT immunocomplexes (Fig. 5*C*). We measured catalytic activity of the anti-FLAG immunoprecipitates using a runoff transcription assay. The 5KR mutant immunocomplexes contained the ability to generate *in vitro* transcripts equal to that of WT immunocomplexes (Fig. 5*D*). Thus, the 5KR mutation of RPB8 constitutes a viable RNA polymerase complex *in vivo* that sustains its polymerase activity. This indicates that RPB8 ubiquitination by BRCA1-BARD1 is not required for RNA polymerase activity.

Ubiquitin-resistant mutant of RPB8 causes UV hypersensitivity. BRCA1 deficiency causes hypersensitivity to DNA damage (14, 26, 27). Because RPB8 is ubiquitinated by BRCA1 after UV irradiation (Fig. 4), it was possible that failure to perform this function could cause the same phenotype. To test this possibility, we established HeLa cell lines that stably express the 5KR mutant of FLAG-RPB8. Two clones each of the WT (WT-1 and WT-2) and of the 5KR (5KR-1 and 5KR-2) cell lines were obtained (Fig. 6*A*). Polyubiquitination of FLAG-RPB8 after UV irradiation was detected in WT cells, but not in mutant cells (Fig. 6*B*). Using these cells, we examined if the expression of the mutant RPB8 affected cell survival after UV irradiation. The cell viabilities of the 5KR clones 48 h after 20 or 35 J/m^2 of UV irradiation were ~38% and 23% of untreated cells at 0 h, respectively, whereas WT clones were ~72% and 53%, respectively (Fig. 6*C*). Parental HeLa cells exhibited viabilities similar to that of WT clones (Fig. 6*C*). Representative data for cells observed by phase contrast microscopy 48 h after UV irradiation (35 J/m^2) and for culture plates stained with Lillie's crystal violet stain are shown (Supplementary Fig. S4). Thus, expression of a ubiquitin-resistant RPB8 form in cells causes UV hypersensitivity.

Because UV-induced cell death is largely ascribable to caspase-induced apoptosis, we next tested whether activation of the caspase pathway by UV irradiation was enhanced in 5KR cells. HeLa cell lines expressing WT or 5KR mutant of FLAG-RPB8 were UV irradiated, and caspase activity was measured by immunoblotting with an antibody to cleaved caspase-3. As shown in Fig. 6*D*, 5KR cells expressed larger amount of cleaved caspase-3 than WT cells did at each time point after UV irradiation. This result suggests that failure to ubiquitinate RPB8 after UV irradiation activates the caspase pathway, resulting in apoptotic cell death.

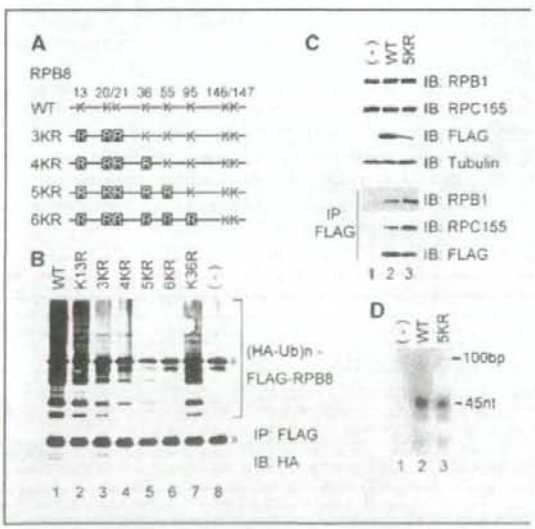

Figure 5. Construction of ubiquitin-resistant RPB8 mutant and assay of its RNA polymerase activity. *A*, the mutant constructs of RPB8. Lys (*K*) residues of RPB8 were substituted with Arg (*R*) as indicated. *B*, Myc-BRCA1$^{1-772}$, BARD1, and HA-ubiquitin were cotransfected into 293T cells either with WT or mutant FLAG-RPB8 as indicated. Polyubiquitination of RPB8 was detected as in Fig. 2*B*. *C*, 293T cells were transfected either with parental pcDNA3 vector (−), WT, or the 5KR mutant of FLAG-RPB8 as indicated. Total cell lysates (*top four panels*) or anti-FLAG immunoprecipitates from equal amounts of total cell lysates (*bottom three panels*) were subjected to immunoblotting with the indicated antibodies. *D*, anti-FLAG immunoprecipitates obtained as in *C* were subjected to an *in vitro* runoff transcription assay using double-stranded DNA templates designed to generate an RNA transcript of 45 nucleotides. Radiolabeled RNA products were resolved by a 12% polyacrylamide/urea gel and scanned with a Typhoon 9400 image analyzer. *, IgG.

Discussion

BRCA1 exists in several different supercomplexes to execute diverse cellular processes. In most of these complexes, BRCA1 exists as a RING heterodimer with BARD1 (28), the form that acquires significant ubiquitin ligase activity (6–8). Revealing the substrates specific for each BRCA1 protein complex is crucial to understand the mechanisms underlying its tumor-suppressor functions.

BRCA1-BARD1 complexes bind to BRCA2 and Rad51 and localize to discrete nuclear foci during S phase. After DNA damage, BRCA1 is phosphorylated by ATM/ATR family kinases (29, 30), and the BRCA1 foci disperse within 30 min (31). The BRCA2-Rad51-containing complex, as well as the BRCA1 complex with Mre11-Rad50-Nbs1, gradually reassemble into different foci (sites of DNA damage) and play important roles in homologous recombination repair. The BRCA1-containing foci begin to appear ~1 h after DNA damage has occurred, reach their peak after 6 to 8 h, and remain until 12 h after damage (31, 32). BRCA1-BARD1 also associates with the RNA polymerase II holoenzyme (15, 16). In contrast to the cases of other complexes described above, BRCA1 dissociates from hyperphosphorylated, processive polymerase II 1 h after DNA damage (17). However, how BRCA1 affects the polymerase II complexes, if at all, during the early stages after DNA damage and before the translocation of BRCA1 to the repair machinery remains to be elucidated. Our results suggest that BRCA1 polyubiquitinates a component of the polymerase II complex, RPB8, at this early stage after DNA damage.

Recently, ubiquitination of phosphorylated RPB1 by BRCA1-BARD1 has been reported (23, 25). Because double knockdown of BRCA1 and BARD1 restored the expression level of the phosphorylated polymerase II that had been repressed by UV irradiation, it was proposed that BRCA1-BARD1 could initiate the degradation of stalled RPB1 (23). However, the BRCA1-BARD1 double knockdown did not detectably affect RPB1 ubiquitination after UV

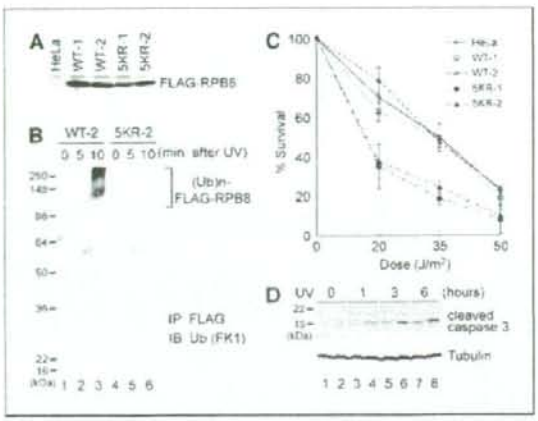

Figure 6. Ubiquitin-resistant RPB8 causes UV hypersensitivity. *A*, cell lysates obtained from two clones each of HeLa cell lines stably expressing either WT (*WT-1* and *WT-2*) or the 5KR mutant (*5KR-1* and *5KR-2*) of FLAG-RPB8 and parental HeLa cells were immunoprecipitated with anti-RPB8 antibody followed by immunoblotting with anti-RPB8 antibody. *B*, HeLa cell lines stably expressing WT (*WT-2, lanes 1–3*) or the 5KR mutant (*5KR-2, lanes 4–6*) of FLAG-RPB8 were UV irradiated (35 J/m^2) and harvested at the indicated times after irradiation. Ubiquitinated RPB8 was detected as described in Fig. 2*B*, except that antipolyubiquitin antibody (*FK1*) was used for immunoblotting. *C*, HeLa cell lines described in *A* were UV irradiated at the indicated doses. Forty-eight hours after irradiation, the cell survival ratio was determined by trypan blue exclusion measurements. The cell number at 0 h (indicated as 0 J/m^2) is 100%. *Points*, mean of measurements carried out in triplicate; *bars*, SD. The experiments were repeated at least twice with similar results. *D*, WT-2 cells (*lanes 1, 3, 5, and 7*) and 5KR-2 cells (*lanes 2, 4, 6, and 8*) were UV irradiated (35 J/m^2) and harvested at the indicated times after irradiation. Whole-cell lysates were immunoblotted with anti–caspase-3 antibody or antitubulin antibody.

irradiation. In addition, BRCA1-BARD1–mediated polyubiquitination of other substrates, including NPM1/B23 and phosphorylated CtIP, is not a signal for degradation (12, 33). Therefore, the restored expression level of the phosphorylated polymerase II by BRCA1-BARD1 double knockdown could be due to an indirect effect (23), for example, through the failure to ubiquitinate RPB8. Nonetheless, the clearly shown *in vitro* ubiquitination of phosphorylated RPB1 by BRCA1-BARD1 (23) strongly supports its direct role. The key to solving this discrepancy may be to analyze the timing of RPB1 ubiquitination *in vivo*. RPB1 ubiquitination shown in the previous report occurred 2 h after UV irradiation, when BRCA1 should already be dissociated from polymerase II and relocalized to the Rad50 or Rad51 DNA repair machineries. It is possible that early after DNA damage, RPB1 and RPB8 are transiently ubiquitinated by BRCA1 at the same time, and it may result in dissociation of the polymerase II holoenzyme from the damaged DNA site. RPB1 ubiquitination and degradation occurring in late phases could be mediated by other E3 ligases, such as the CSA-DDB1-CUL4A-ROC1 complex (34, 35).

It is well known that cells with impaired BRCA1 function display hypersensitivity to a range of DNA-damaging agents, including IR and UV irradiation (3, 26). However, the mechanism underlying this phenomenon is not fully understood. Although the failure of checkpoint function is a possible mechanism responsible for the hypersensitivity, it has been reported that neither selective abrogation of the S-phase checkpoint nor the G_2 checkpoint itself results in decreased cell survival after DNA damage (36, 37). Therefore, it has been proposed that some function of BRCA1 other than S-phase or G_2 cell cycle control may affect cell survival after DNA damage (37). The UV hypersensitivity of the cells stably expressing a ubiquitin-resistant mutant of RPB8 shown in this report provides a possible new role for BRCA1 that may compensate for this theoretical defect. Because hyperphosphorylated stalled polymerase II at damaged sites is an extremely cytotoxic ramification of DNA damage (38), the observed UV hypersensitivity could be caused by trapped polymerase II or prolonged polymerase II hyperphosphorylation. In this process, the ubiquitination of RPB8 could be an important step either for polymerase II disassembly, polymerase II dissociation from DNA, or polymerase II dephosphorylation by FCP1. It is interesting that there is considerable expression of endogenous WT RPB8 in the ubiquitin-resistant RPB8 mutant cells (Fig. 4*A*). This indicates that only partial interference of the RNA polymerase recovery is enough to induce cell death, probably by silencing a gene critical for cell survival. Alternatively, polymerase II complexes containing mutant RPB8 could stall at the damaged sites, subsequently causing a gridlock of all polymerase II complexes, including WT complexes. Supporting this idea, induction of local damage by microbeam UV irradiation in the nucleus led to transcription inhibition throughout the nucleus (39).

Lastly, it is noteworthy that RPB8 is shared by all three classes of RNA polymerases (19, 40). Whereas polymerase II synthesizes mRNA, which is only ~ 5% of all RNAs, polymerase I and polymerase III synthesize the remaining 95% of all RNAs. Therefore, modification of those complexes, rather than polymerase II, might enormously influence cellular conditions. Whereas RPB1 has been intensively studied, the role of RPB8 in the DNA damage response has been poorly understood. The ubiquitination of RPB8 by BRCA1 reported here provides additional evidence for the role of RNA polymerases in the DNA damage response as well as in carcinogenesis.

Acknowledgments

Received 8/31/2006; revised 11/15/2006; accepted 11/30/2006.

Grant support: Japan Society for the Promotion of Science and the Japanese Ministry of Education, Culture, Sports, Science and Technology.

The costs of publication of this article were defrayed in part by the payment of page charges. This article must therefore be hereby marked *advertisement* in accordance with 18 U.S.C. Section 1734 solely to indicate this fact.

We thank Drs. Yanping Zhang, Minoru Takata, and Masamichi Ishiai for helpful discussions and critical reading of the manuscript; and Drs. Richard Baer and Nouria Hernandez for their generous contribution of materials.

References

1. Turner N, Tutt A, Ashworth A. Hallmarks of "BRCA-ness" in sporadic cancers. Nat Rev Cancer 2004;4:814–9.
2. Deng CX. Roles of BRCA1 in centrosome duplication. Oncogene 2002;21:6222–7.
3. Venkitaraman AR. Cancer susceptibility and the functions of BRCA1 and BRCA2. Cell 2002;108:171–82.
4. Zheng L, Li S, Boyer TG, Lee WH. Lessons learned from BRCA1 and BRCA2. Oncogene 2000;19:6159–75.
5. Baer R, Ludwig T. The BRCA1/BARD1 heterodimer, a tumor suppressor complex with ubiquitin E3 ligase activity. Curr Opin Genet Dev 2002;12:86–91.
6. Brzovic PS, Keeffe JR, Nishikawa H, et al. Binding and recognition in the assembly of an active BRCA1/BARD1 ubiquitin-ligase complex. Proc Natl Acad Sci U S A 2003;100:5646–51.
7. Hashizume R, Fukuda M, Maeda I, et al. The RING heterodimer BRCA1-1 is a ubiquitin ligase inactivated by a breast cancer-derived mutation. J Biol Chem 2001;276:14537–40.
8. Mallery DL, Vandenberg CJ, Hiom K. Activation of the E3 ligase function of the BRCA1/BARD1

complex by polyubiquitin chains. EMBO J 2002;21:6755–62.
9. Chau V, Tobias JW, Bachmair A, et al. A multiubiquitin chain is confined to specific lysine in a targeted short-lived protein. Science 1989;243:1576–83.
10. Morris JR, Solomon E. BRCA1: BARD1 induces the formation of conjugated ubiquitin structures, dependent on K6 of ubiquitin, in cells during DNA replication and repair. Hum Mol Genet 2004;13:807–17.
11. Nishikawa H, Ooka S, Sato K, et al. Mass spectrometric and mutational analyses reveal Lys-6-linked polyubiquitin chains catalyzed by BRCA1-1 ubiquitin ligase. J Biol Chem 2004;279:3916–24.
12. Sato K, Hayami R, Wu W, et al. Nucleophosmin/B23 is a candidate substrate for the BRCA1–1 ubiquitin ligase. J Biol Chem 2004;279:30919–22.
13. Wu-Baer F, Lagrazon K, Yuan W, Baer R. The BRCA1/BARD1 heterodimer assembles polyubiquitin chains through an unconventional linkage involving lysine residue K6 of ubiquitin. J Biol Chem 2003;278:34743–6.
14. Ruffner H, Joazeiro CA, Hemmati D, Hunter T, Verma IM. Cancer-predisposing mutations within the RING domain of BRCA1: loss of ubiquitin protein ligase activity and protection from radiation hypersensitivity. Proc Natl Acad Sci U S A 2001;98:5134–9.
15. Chiba N, Parvin JD. The BRCA1 and BARD1 association with the RNA polymerase II holoenzyme. Cancer Res 2002;62:4222–8.
16. Scully R, Anderson SF, Chao DM, et al. BRCA1 is a component of the RNA polymerase II holoenzyme. Proc Natl Acad Sci U S A 1997;94:5605–10.
17. Krum SA, Miranda GA, Lin C, Lane TF. BRCA1 associates with processive RNA polymerase II. J Biol Chem 2003;278:52012–20.
18. Lane TF. BRCA1 and transcription. Cancer Biol Ther 2004;3:528–33.
19. Shpakovski GV, Acker J, Wintzerith M, Lacroix JF, Thuriaux P, Vigneron M. Four subunits that are shared by the three classes of RNA polymerase are functionally interchangeable between *Homo sapiens* and *Saccharomyces cerevisiae*. Mol Cell Biol 1995;15:4702–10.
20. Boulton SJ. BRCA1-mediated ubiquitylation. Cell Cycle 2006;5:1481–6.
21. Kirkpatrick DS, Hathaway NA, Hanna J, et al. Quantitative analysis of *in vitro* ubiquitinated cyclin B1 reveals complex chain topology. Nat Cell Biol 2006;8:700–10.
22. Bregman DB, Halaban R, van Gool AJ, Henning KA, Friedberg EC, Warren SL. UV-induced ubiquitination of RNA polymerase II: a novel modification deficient in Cockayne syndrome cells. Proc Natl Acad Sci U S A 1996;93:11586–90.
23. Kleiman FE, Wu-Baer F, Fonseca D, Kaneko S, Baer R, Manley JL. BRCA1/BARD1 inhibition of mRNA 3′ processing involves targeted degradation of RNA polymerase II. Genes Dev 2005;19:1227–37.
24. Ratner JN, Balasubramanian B, Corden J, Warren SL, Bregman DB. Ultraviolet radiation-induced ubiquitination and proteasomal degradation of the large subunit of RNA polymerase II. Implications for transcription-coupled DNA repair. J Biol Chem 1998;273:5184–9.
25. Starita LM, Horwitz AA, Keogh MC, Ishioka C, Parvin JD, Chiba N. BRCA1/BARD1 ubiquitinate phosphorylated RNA polymerase II. J Biol Chem 2005;280:24498–505.
26. Abbott DW, Thompson ME, Robinson-Benion C, Tomlinson G, Jensen RA, Holt JT. BRCA1 expression restores radiation resistance in BRCA1-defective cancer cells through enhancement of transcription-coupled DNA repair. J Biol Chem 1999;274:18808–12.
27. Shen SX, Weaver Z, Xu X, et al. A targeted disruption of the murine Brca1 gene causes γ-irradiation hypersensitivity and genetic instability. Oncogene 1998;17:3115–24.
28. Greenberg RA, Sobhian B, Pathania S, Cantor SB, Nakatani Y, Livingston DM. Multifactorial contributions to an acute DNA damage response by BRCA1/BARD1-containing complexes. Genes Dev 2006;20:34–46.
29. Cortez D, Wang Y, Qin J, Elledge SJ. Requirement of ATM-dependent phosphorylation of brca1 in the DNA damage response to double-strand breaks. Science 1999;286:1162–6.
30. Tibbetts RS, Cortez D, Brumbaugh KM, et al. Functional interactions between BRCA1 and the checkpoint kinase ATR during genotoxic stress. Genes Dev 2000;14:2989–3002.
31. Scully R, Chen J, Ochs RL, et al. Dynamic changes of BRCA1 subnuclear location and phosphorylation state are initiated by DNA damage. Cell 1997;90:425–35.
32. Zhong Q, Chen CF, Li S, et al. Association of BRCA1 with the hRad50-hMre11-p95 complex and the DNA damage response. Science 1999;285:747–50.
33. Yu X, Fu S, Lai M, Baer R, Chen J. BRCA1 ubiquitinates its phosphorylation-dependent binding partner CtIP. Genes Dev 2006;20:1721–6.
34. Groisman R, Polanowska J, Kuraoka I, et al. The ubiquitin ligase activity in the DDB2 and CSA complexes is differentially regulated by the COP9 signalosome in response to DNA damage. Cell 2003;113:357–67.
35. Hu J, McCall CM, Ohta T, Xiong Y. Targeted ubiquitination of CDT1 by the DDB1–4A-ROC1 ligase in response to DNA damage. Nat Cell Biol 2004;6:1003–9.
36. Xu B, Kim ST, Lim DS, Kastan MB. Two molecularly distinct G(2)/M checkpoints are induced by ionizing irradiation. Mol Cell Biol 2002;22:1049–59.
37. Xu B, O'Donnell AH, Kim ST, Kastan MB. Phosphorylation of serine 1387 in Brca1 is specifically required for the Atm-mediated S-phase checkpoint after ionizing irradiation. Cancer Res 2002;62:4588–91.
38. van den Boom V, Jaspers NG, Vermeulen W. When machines get stuck-obstructed RNA polymerase II: displacement, degradation or suicide. Bioessays 2002;24:780–4.
39. Takeda S, Naruse S, Yatani R. Effects of ultra-violet microbeam irradiation of various sites of HeLa cells on the synthesis of RNA, DNA and protein. Nature 1967;213:696–7.
40. Briand JF, Navarro F, Rematier P, et al. Partners of Rpb8p, a small subunit shared by yeast RNA polymerases I, II and III. Mol Cell Biol 2001;21:6056–65.

Regulatory Roles of NKT Cells in the Induction and Maintenance of Cyclophosphamide-Induced Tolerance[1]

Toshiro Iwai,* Yukihiro Tomita,[2]* Shinji Okano,[†] Ichiro Shimizu,* Yohichi Yasunami,[‡] Takashi Kajiwara,* Yasunobu Yoshikai,[§] Masaru Taniguchi,[‖] Kikuo Nomoto,[¶] and Hisataka Yasui*

We have previously reported the sequential mechanisms of cyclophosphamide (CP)-induced tolerance. Permanent acceptance of donor skin graft is readily induced in the MHC-matched and minor Ag-mismatched recipients after treatment with donor spleen cells and CP. In the present study, we have elucidated the roles of NKT cells in CP-induced skin allograft tolerance. BALB/c AnNCrj (H-2^d, Lyt-1.2, and Mls-1^b) wild-type (WT) mice or Vα14 NKT knockout (KO) (BALB/c) mice were used as recipients, and DBA/2 NCrj (H-2^d, Lyt-1.1, and Mls-1^a) mice were used as donors. Recipient mice were primed with 1×10^8 donor SC i.v. on day 0, followed by 200 mg/kg CP i.p. on day 2. Donor mixed chimerism and permanent acceptance of donor skin allografts were observed in the WT recipients. However, donor skin allografts were rejected in NKT KO recipient mice. In addition, the donor reactive Vβ6$^+$ T cells were observed in the thymus of a NKT KO recipient. Reconstruction of NKT cells from WT mice restored the acceptance of donor skin allografts. In addition, donor grafts were partially accepted in the thymectomized NKT KO recipient mice. Furthermore, the tolerogen-specific suppressor cell was observed in thymectomized NKT KO recipient mice, suggesting the generation of regulatory T cells in the absence of NTK cells. Our results suggest that NKT cells are essential for CP-induced tolerance and may have a role in the establishment of mixed chimerism, resulting in clonal deletion of donor-reactive T cells in the recipient thymus. *The Journal of Immunology*, **2006, 177: 8400–8409.**

Natural killer T cells, which are characterized by coexpression of NK cell receptors and a single invariant T cell Ag receptor encoded by *Vα14* and *Jα281* gene segments, have been identified as a novel lymphoid lineage distinct from conventional T cells or NK cells. Although the physiological roles of NKT cells remain obscure, Vα14 NKT cells have been demonstrated to play important roles in tumor immunity (1), autoimmune disease (2), and infectious immunity (3, 4) via the dominant production of Th1 cytokine γ-IFN and Th2 cytokine IL-4. Regarding transplantation immunity, two reports have suggested a regulatory role of NKT cells in both allogeneic and xenogeneic tolerance systems induced by mAbs (5, 6).

Since 1982, we have investigated cyclophosphamide (CP)[3]-induced tolerance that consists of an i.v. injection of 1×10^8 allogeneic spleen cells (SC) (day 0) followed by i.p. administration of 200 mg/kg CP on day 2 (7–18). By using this method, we were able to readily induce long-lasting skin allograft tolerance in most H-2-matched combinations (10–12), but not in fully H-2-mismatched combinations (7, 13). Our previous studies have elucidated the three major mechanisms involved using H-2-compatible, Mls-1^a-disparate combinations and Mls-1^a Ag-reactive Vβ6$^+$ T cells (11–14). The first is the destruction of Ag-stimulated and then proliferating T cells in the periphery by CP treatment. CD4$^+$Vβ6$^+$ T cells proliferated and then disappeared in the periphery of the recipients tolerized to H-2-compatible, Mls-1^a-disparate Ags. The second, at 4–6 wk after the treatments, is the establishment of intrathymic chimerism at both the thymocyte and dendritic cell levels, followed by the clonal deletion of Vβ6$^+$ T cells that begins in the thymus. The third mechanism is the generation of regulatory cells in the late stage of tolerance.

The aim of the present study was to investigate the regulatory role of NKT cells in our CP-induced tolerance system by using Vα14 NKT knockout (KO) mice. Although an essential role for NKT cells in the induction of transplantation tolerance has been suggested in two previous reports (5, 6), the detailed mechanisms have not been clarified. Here, we evaluated the role of NKT cells in our three important mechanisms, i.e., clonal destruction, intrathymic clonal deletion, and generation of regulatory cells. The results clearly showed that NKT cells were essential for CP-induced tolerance through the establishment of intrathymic clonal deletion. Without NKT cell-mediated immunoregulation, however, our results demonstrated that the generation of regulatory cells for the maintenance of tolerance in the late stage of tolerance can occur, in addition to clonal destruction at the early stage.

Materials and Methods

Animals

Inbred mice of the BALB/c AnNCrj (H-2^d, Lyt-1.2, and Mls-1^b) and DBA/2 NCrj (H-2^d, Lyt-1.1, and Mls-1^a) strains were obtained from

*Department of Cardiovascular Surgery and [†]Division of Pathophysiological and Experimental Pathology, Department of Pathology, Graduate School of Medical Sciencies, Kyushu University, Fukuoka, Japan; [‡]Department of Surgery 1, Fukuoka University School of Medicine, Fukuoka, Japan; [§]Department of Infection Control and [¶]Department of Immunology, Medical Institute of Bioregulation, Kyushu University, Fukuoka, Japan; and [‖]Laboratory for Immune Regulation, RIKEN Research Center for Allergy and Immunology, Yokohama, Japan

Received for publication March 18, 2004. Accepted for publication September 22, 2006.

The costs of publication of this article were defrayed in part by the payment of page charges. This article must therefore be hereby marked *advertisement* in accordance with 18 U.S.C. Section 1734 solely to indicate this fact.

[1] This study was supported by a Grant-in-Aid for Scientific Research from the Ministry of Health and Welfare, Japan (to Y.T.). Y.T. was also the recipient of a Surgical Research Foundation Grant from the Japanese Surgical Association.

[2] Address correspondence and reprint requests to Dr. Yukihiro Tomita, Department of Cardiovascular Surgery, Graduate School of Medical Sciences, Kyushu University, 3-1-1 Maidashi, Higashi-ku, Fukuoka 812-8582, Japan. E-mail address: tomita@heart.med.kyushu-u.ac.jp

[3] Abbreviations used in this paper: CP, cyclophosphamide; αGalCer, α-galactosyl ceramide; BMC, bone marrow cell; Gy, gray; KO, knockout; LMNC, liver mononuclear cell; MST, mean survival time; SC, spleen cell; WBC, white blood cell; WT, wild type.

0022-1767/06/$02.00

Charles River Laboratories. Inbred mice of the B10.D2 SnSlc ($H\text{-}2^d$) strain were obtained from Japan SLC. Jα281 KO (Vα14 NKT KO) mice with a BALB/c background were also used as recipients (1). The recipients were used at 12–16 wk of age. All animals received humane care in compliance with the Guidelines for Animal Experiments of Kyushu University and Law no. 105 and Notification no. 6 of the Japanese government.

Cell preparation

Mice were sacrificed by decapitation. The spleens were collected and kept on ice in RPMI 1640 medium (Invitrogen Life Technologies) supplemented with antibiotics (100 μg/ml penicillin and 100 μg/ml streptomycin). Spleens were disrupted in the medium by pressing spleen fragments between two glass slides. Cell suspensions were filtered through cotton gauze and washed three times with the RPMI 1640 medium. Viable nucleated cells were counted and usually adjusted to 20×10^7/ml.

Conditioning of CP-induced tolerance

A 0.5-ml aliquot containing 1×10^8 SC from DBA/2 mice was injected into the tail vein of recipient BALB/c mice. Two days later, CP (Endoxan; Shionogi) dissolved in PBS at a concentration of 10 mg/ml was injected i.p. at a dose of 200 mg/kg. The day of the injection of DBA/2 SC is referred to as day 0 throughout this report.

Reconstitution of NKT cells in NKT KO mice

We set up two methods to reconstitute NKT cells in NKT KO mice. First, a 0.5-ml aliquot containing 1×10^8 SC from WT mice (containing ~1% NKT cells) was injected into the tail vein of recipient NKT KO mice on day −7. Second, recipient NKT KO mice were irradiated with three gray (Gy) on day −28 and then reconstituted with 1×10^7 SC and 5×10^6 untreated bone marrow cells (BMC) (containing ~0.1–0.4% NKT cells) from WT mice on the same day. The preparation of BMC was performed according to a previous method (19). Briefly, the bone marrow in the femoral and tibial bones was flushed out using a 5-ml syringe with a 26-gauge needle (Terumo).

Skin grafting

Skin grafting was performed using our previously reported procedure (20). Briefly, a square, full-thickness skin graft (1 cm^2) was prepared on the right lateral thoracic wall of the recipient mouse. The graft was fixed to the graft bed with eight interrupted sutures of 5-0 silk thread and covered with protective tape. The first inspection was conducted on the 7th day, followed by daily inspection for 3 wk. Grafts were considered as rejected at the time of complete sloughing or when they formed a dry scar. Survival was expressed as the median survival time and the mean survival time (MST) ± SD.

Thymectomy

Recipients were anesthetized with phenobarbital (Nembutal) at 50 mg/kg administered i.p. After a partial sternotomy, the thymectomy was performed by en bloc excision using two pairs of forceps (21). The absence of thymic tissue was always confirmed when the thymectomized animals were sacrificed, and animals showing the presence of residual thymic tissue were excluded from the analysis.

Flow cytometry

Phenotyping was performed at various times, beginning 2 wk after the injection of SC. Recipients were tail bled and white blood cells (WBC) were prepared by hypotonic shock (21). In some experiments, SC and thymocytes were used for chimeric assays. Staining with both donor-specific and T cell-specific mAbs was performed on each recipient and control mouse. Cells were incubated with a PE-conjugated anti-Lyt-1 (Lyt-1.1 and Lyt-1.2) (BD Pharmingen) mAb and a FITC-conjugated Lyt-1.1 (BD Pharmingen) mAb for 30 min at 4°C and then washed twice. To block nonspecific FcγR binding of labeled Abs, 10 μl of an undiluted culture supernatant of 2.4G2 (rat anti-mouse FcγR mAb) was used. All data were analyzed with a FACScan (BD Biosciences). Dead cells were excluded by gating out low forward scatter, high propidium iodide-retaining cells.

For the analysis of TCR expression on T cells of SC or WBC, two-color analysis was performed (21). WBC or SC were labeled with FITC-conjugated anti-Vβ6 or Vβ8.1/8.2 mAb (BD Pharmingen), and PE-conjugated anti-CD4 (BD Pharmingen) mAb. To determine the percentage of $CD4^+$ T cells that were $V\beta6^+$ or $V\beta8.1/8.2^+$, 10,000–20,000 gated $CD4^+$ cells were collected. For the analysis of TCR expression on thymocytes, three-color analysis was performed (21). Thymocytes were labeled with FITC-conjugated anti-Vβ6 or Vβ8.1/8.2 mAb (BD Pharmingen), PE-conjugated anti-CD4 (BD Pharmingen) mAb, and allophycocyanin-conjugated anti-CD8 (BD Pharmingen) mAb for 30 min at 4°C. To determine the percentage of CD4 single-positive cells that were $V\beta6^+$ or $V\beta8.1/8.2^+$, 5,000 to 10,000 gated $CD4^+$ and $CD8^-$ cells were collected. We investigated the effect of SC/CP on the ratio of $CD4^+V\beta6^+$ T cell or $CD4^+V\beta8^+$ T cell subsets to the total $CD4^+$ T cell number in the spleen or WBC and on the ratio of $CD4^+CD8^-V\beta6^+$ T cell or $CD4^+CD8^-V\beta8^+$ T cell subsets to the total $CD4^+CD8^-$ T cell number in the thymus. We also investigated the effect of SC/CP on the absolute number of $CD4^+V\beta6^+$ T cells or $CD4^+V\beta8^+$ T cells in the spleen and thymus.

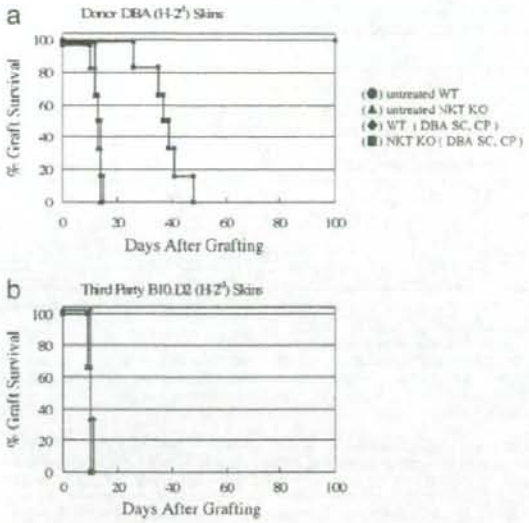

FIGURE 1. Skin allograft survival in the recipient BALB/c mice treated with DBA/2 SC. Recipient mice were grafted with skin from donor DBA/2 (DBA) (*a*) or third party B10.D2 (*b*) mice 4 wk after treatment. *a*. The groups and median skin graft survival times were as follows: ●, Untreated WT mice ($n = 6$; 13.5 days); ▲, untreated NKT KO mice ($n = 6$; 13 days); ◆, WT mice treated with DBA/2 SC and CP ($n = 6$; >100 days); and ■, NKT KO mice treated with DBA/2 SC and CP ($n = 6$; 38 days). *b*. B10.D2 skin grafts were rejected within 14 days after grafting in the following groups: ◆, WT mice treated with DBA/2 SC and CP ($n = 3$); ■, NKT KO mice treated with DBA/2 SC and CP ($n = 3$).

For the staining of NKT cells, SC or liver mononuclear cells (LMNC) were stained with PE-conjugated α-galactosyl ceramide (αGalCer)/CD1d tetramers and FITC-conjugated anti-CD3 mAb (BD Pharmingen). PE-conjugated αGalCer/CD1d tetramers were prepared as previously described (22). The liver was disrupted in RPMI 1640 medium (Invitrogen Life Technologies) supplemented with 10% FCS by pressing liver fragments between two glass slides and then washed, resuspended in a 40% isotonic Percoll solution (Amersham Biosciences) and underlaid with a 67.5% isotonic Percoll solution. Centrifugation for 30 min at 3,000 rpm at room temperature isolated the LMNC at the interface. Cells were washed two times with HBSS containing 2% FCS and resuspended in the same solution.

Adoptive transfer experiment

To elucidate the existence of regulatory cells in the tolerant recipients, adoptive transfer experiments were performed as described previously (14). Briefly, 1×10^8 or 4×10^7 SC from the recipient mice accepting DBA/2 skin allografts for over 100 days were transferred into WT mice that had been irradiated with 3 Gy on the same day. The SC were harvested from WT or NKT mice that had been thymectomized and treated with DBA/2 SC and CP. Skin grafting was performed 1 day following the adoptive transfer. In one experiment, $CD4^+CD8^+Thy1.2^+$ T cell depletion was performed using anti-CD4 mAb (L3/T4), anti-CD8 mAb (Ly2.2) (Cedarlane Laboratories), anti-Thy-1.2 mAb (Meiji), and complement (Low-Tox-M rabbit complement; Cedarlane Laboratories).

Table 1. *Chimerism and clonal destruction in WBC of recipients treated with DBA/2 SC and CP[a]*

Group	Recipient	Treatment[a] SC (day 0)	Treatment[a] CP (day 2)	No. of Mice	Chimeric Analysis (percent positive cells ± SD) Lyt-1.1⁺/Lyt-1⁺ (%) 2 wk	Lyt-1.1⁺/Lyt-1⁺ (%) 8 wk	Analysis of TCR Expression (percent positive cells ± SD) CD4⁺Vβ6⁺/CD4⁺ (%) 3 wk	CD4⁺Vβ6⁺/CD4⁺ (%) 9 wk	CD4⁺Vβ6⁺/CD4⁺ (%) 3 wk	CD4⁺Vβ6⁺/CD4⁺ (%) 9 wk
1	BALB/c WT	(−)	(−)	6	0		10.7 ± 1.2		16.6 ± 1.6	
2	BALB/c NKT KO	(−)	(−)	6	0		11.3 ± 1.4		12.2 ± 1.7	
3	DBA/2	(−)	(−)	6	96.3 ± 2.4		0		13.0 ± 1.1	
4	BALB/c WT	DBA/2	200[b]	6	2.6 ± 0.8[c]	3.8 ± 1.0[c]	1.6 ± 0.5	1.1 ± 0.4	17.1 ± 1.9	16.6 ± 2.0
5	BALB/c NKT KO	DBA/2	200[b]	6	1.5 ± 0.1	0.9 ± 0.2	1.3 ± 0.3	0.8 ± 0.2	12.9 ± 1.2	2.6 ± 1.7

[a] The recipient mice were primed i.v. with 1×10^8 viable DBA/2 SC on day 0 and then given 200 mg/kg CP on day 2.
[b] Milligrams per kilogram (mg/kg).
[c] $p < 0.01$ compared with group 5.

Statistics

The statistical significance of the data was determined by a Mann-Whitney *U* test when the data were nonparametric or a Student's *t* test when the data were parametric. A value of $p < 0.05$ was considered to be statistically significant.

Results

Skin allograft prolongation in H-2-matched DBA/2 (H-2^d) → BALB/c WT (H-2^d) or BALB/c background Vα14 NKT KO (H-2^d) combination mice by using 1×10^8 DBA/2 SC followed by 200 mg/kg CP

When BALB/c WT (H-2^d) or BALB/c background NKT KO mice were grafted with H-2-matched DBA/2 skin allografts (H-2^d), the DBA/2 grafts were rejected within 14 days following grafting (Fig. 1*a*). Similarly, DBA/2 skin grafts were rejected within 14 days in BALB/c WT or NKT KO mice treated with DBA/2 SC alone or 200 mg/kg CP alone (data not shown). All of the DBA/2 skin allografts survived for >100 days in the recipient BALB/c WT mice treated with DBA/2 SC followed by CP ($n = 6$; MST, >100 days). When syngeneic (BALB/c) WT SC or PBS (0.5 ml) was used instead of DBA/2 SC or CP, respectively, the survival times of DBA/2 skin grafts were not prolonged (data not shown). In contrast, all DBA/2 skin grafts were rejected within 48 days in the recipient NKT KO mice treated with DBA/2 SC followed by CP ($n = 6$; MST, 38 days), although the survival of the grafts was moderately prolonged. The skin allograft prolongation in both BALB/c WT mice and NKT KO mice, which were treated with DBA/2 SC followed by CP, was tolerogen-specific, because the third party skin grafts of the B10.D2 strain (H-2^d) were rejected in a normal fashion (Fig. 1*b*).

Chimerism and reduction of Mls-1^a-reactive CD4$^+$Vβ6$^+$ T cells of WBC in the recipient mice treated with DBA/2 SC plus CP

As we previously reported (14), a minimal degree of mixed chimerism was detected in the BALB/c WT (Lyt-1.2) mice made tolerant of DBA/2 (Lyt-1.1) skin allografts. The mixed chimeric state induced with DBA/2 SC and CP was examined using

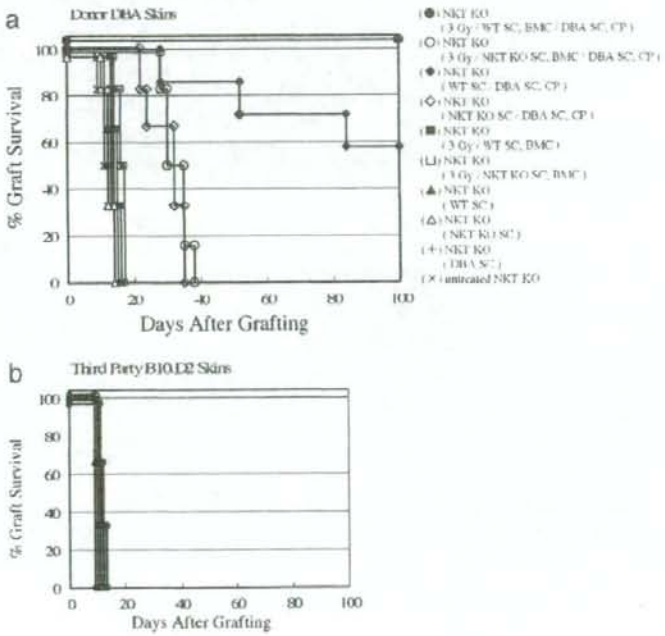

FIGURE 2. Skin allograft survival in recipient BALB/c NKT KO mice reconstituted with NKT cells and treated with DBA/2 SC and CP. Recipient mice were grafted with skin from donor DBA/2 (DBA) (*a*) or third party B10.D2 (*b*) mice 4 wk after treatment. *a* The groups and median skin graft survival times were as follows: ●, NKT KO mice irradiated with 3 Gy followed by reconstitution with WT SC and BMC and treatment with DBA/2 SC and CP ($n = 6$; >100 days); ○, NKT KO mice irradiated with 3 Gy followed by reconstitution with NKT KO SC and BMC and treatment with DBA/2 SC and CP ($n = 6$; 32.5 days); ◆, NKT KO mice reconstituted with WT SC and treated with DBA/2 SC and CP ($n = 7$; >100 days); ◇, NKT KO mice reconstituted with NKT KO SC and treated with DBA/2 SC and CP ($n = 6$; 32 days); ■, NKT KO mice irradiated with 3 Gy followed by reconstitution with WT SC and BMC ($n = 6$; 15 days); □, NKT KO mice irradiated with 3 Gy followed by reconstitution with NKT KO SC and BMC ($n = 6$; 16.5 days); ▲, NKT KO mice reconstituted with WT SC ($n = 6$; 13 days); △, NKT KO mice reconstituted with NKT KO SC ($n = 6$; 12 days); +, NKT KO mice treated with DBA/2 SC alone ($n = 6$; 14 days); and ×, untreated NKT KO mice ($n = 6$; 11.5 days). *b*, B10.BR skin grafts were rejected within 14 days after grafting in all of the groups described above in *a* ($n = 3$ in each group).

PE-conjugated anti-Lyt-1 (Lyt-1.1 and Lyt-1.2) mAb and FITC-conjugated Lyt-1.1 mAb. WBC were obtained from the recipient mice at 2 and 8 wk after tolerance induction (Table I).

In the T (Lyt-1$^+$) cells of BALB/c WT mice treated with DBA/2 SC and CP (Table I; group 4), 2–4% of Lyt-1.1 cells were clearly detected in the recipient WBC after tolerance induction. In contrast, a lower degree of chimerism was clearly detected at 2 wk (mean ± SD, 1.5 ± 0.1; $p < 0.01$ compared with group 4) and became <1% at 8 wk in the T (Lyt-1$^+$) cells of NKT KO mice treated with DBA/2 SC followed by CP (Table I; group 5). A higher degree of chimerism was always observed in recipient BALB/c WT mice treated with DBA/2 SC and CP. These results were reproducible in five independent experiments (data not shown).

We examined the expression of the Mls-1^a-reactive TCR Vβ6 in BALB/c WT or NKT KO (Mls-1^b) mice treated with DBA/2 (Mls-1^a) SC and CP. The WBC from the recipients were stained with FITC-conjugated anti-Vβ6 mAb and PE-conjugated anti-CD4 mAb (Table I).

In the WBC of untreated BALB/c WT or NKT KO mice, CD4$^+$Vβ6$^+$ T cells were detected (Table I; group 1 or 2, respectively), whereas they were hardly detected in the WBC of untreated DBA/2 mice (Table I; group 3). In all of the BALB/c WT mice treated with DBA/2 SC and CP (Table I; group 4), CD4$^+$Vβ6$^+$ T cells were significantly reduced by 3 wk. The same results were obtained in the WBC of NKT KO mice treated with DBA/2 SC and CP (Table I; group 5). There was no statistically significant difference in the results between groups 4 and 5. The disappearance of T cells from the WBC was specific for Vβ6$^+$ T cells, because the percentage of Vβ8.1/8.2$^+$ T cells was not significantly altered.

Induction of DBA/2 skin graft prolongation in NKT KO mice reconstituted with NKT cells from BALB/c WT mice

To clarify whether NKT cells were involved in the limitation of skin graft tolerance in CP-induced tolerance, NKT cells were reconstituted in NKT KO mice (Fig. 2). When SC and LMNC were stained with PE-conjugated αGalCer/CD1d tetramers and FITC-conjugated anti-CD3 mAb, αGalCer/CD1d tetramer$^+$CD3$^+$ cells accounted for ~1.0 ± 0.3 and 19.5 ± 5.4% of SC and LMNC in untreated BALB/c WT mice ($n = 3$), respectively, and 0.3 ± 0.1 and 1.2 ± 0.2% of SC and LMNC in untreated NKT KO mice ($n = 3$), respectively. A small percentage of αGalCer/CD1d tetramer$^+$CD3$^+$ cells were detected in NKT KO mice, because the NKT KO mice used in this study were generated by disruption of the *Jα281* gene (1). In contrast, αGalCer/CD1d tetramer$^+$CD3$^+$ cells accounted for ~0.4 ± 0.1 and 4.3 ± 0.5% in SC and LMNC of NKT KO mice ($n = 3$) injected with BALB/c WT SC 7 days earlier, respectively. Therefore, we planned an additional experiment to further reconstitute NKT cells in NKT KO mice. For this purpose, recipient NKT KO mice were irradiated with 3 Gy on day −28 and then injected with 1×10^7 SC and 5×10^6 untreated BMC from WT mice on the same day. In NKT KO mice ($n = 5$) irradiated and injected with BALB/c WT SC and BMC 28 days earlier, αGalCer/CD1d tetramer$^+$CD3$^+$ cells accounted for ~0.7 ± 0.1 and 9.5 ± 2.6% of SC and LMNC, respectively. When NKT KO mice were injected with 1×10^8 SC from BALB/c WT mice on day −7 and treated with SC on day 0 and CP on day 2, the survival of DBA/2 skin grafts was significantly prolonged ($n = 7$; MST, >100 days), and four of seven recipients accepted donor DBA/2 skin grafts for >100 days (Fig. 2*a*). DBA/2 skin grafts were accepted for >100 days in all of the NKT KO mice irradiated with 3 Gy on day −28, reconstituted with 1×10^7 SC and 5×10^6 BMC from BALB/c WT mice on day −28, and then treated with DBA/2 SC on day 0 and CP on day 2 (Fig. 2*a*). Survival of donor skin grafts was not significantly prolonged in NKT KO mice reconstituted with SC and/or BMC from NKT KO mice and treated with DBA/2 SC and CP as compared with that for NKT KO mice treated with DBA/2 SC and CP. In contrast, no skin graft prolongation was observed in NKT KO mice reconstituted with BALB/c WT SC or BMC, irradiated NKT KO mice reconstituted with BALB/c WT SC and BMC, NKT KO mice reconstituted with NKT KO SC or BMC, or irradiated NKT KO mice reconstituted with NKT SC and BMC if the recipient mice were not treated with donor SC and CP (Fig. 2*a*). This skin allograft prolongation was tolerogen-specific, because the third party skin of the B10.D2 strain (H-2^d) was rejected in a normal fashion (Fig. 2*b*).

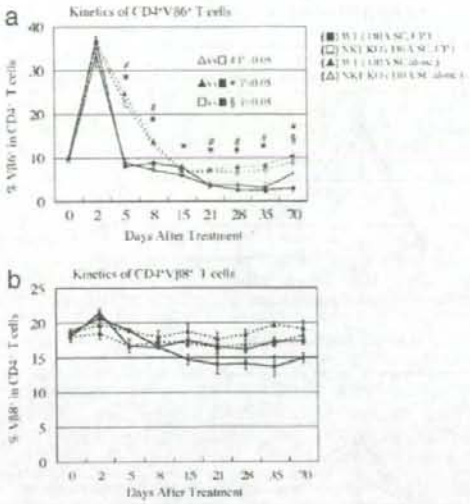

FIGURE 3. Clonal destruction in the periphery of recipient mice. The kinetics of CD4$^+$Vβ6$^+$ (*a*) or CD4$^+$Vβ8.1/8.2$^+$ (*b*) T cells in spleen cells harvested from the recipient mice are shown. SC were labeled with FITC-conjugated anti-Vβ6 or Vβ8.1/8.2 mAb and PE-conjugated anti-CD4 mAb. To determine the percentage of CD4$^+$ T cells that were Vβ6$^+$ or Vβ8.1/8.2$^+$, 10,000–20,000 gated CD4$^+$ cells were collected. SC cells were obtained from WT (H-2^d; Mls-1^b) mice treated with DBA/2 (DBA) (H-2^d; Mls-1^a) SC and CP (■; $n = 4$), NKT KO mice treated with DBA/2 SC and CP (□; $n = 4$), WT mice treated with DBA/2 SC alone (▲; $n = 4$), and NKT KO mice treated with DBA/2 SC alone (△; $n = 4$). Vertical bars represent the SD. The statistical significance of the differences among groups was analyzed and the results are given in *a*.

Analysis of splenic clonal destruction and intrathymic clonal deletion and mixed chimerism in BALB/c WT or NKT KO mice treated with DBA/2 SC and CP

As reported previously (12, 13), the induction mechanism of CP-induced tolerance is the clonal destruction of Ag-stimulated and proliferating T cells by the antimitotic drug CP. To further analyze the role of NKT cells in the tolerance induction, we examined the kinetics of Mls-1^a-reactive CD4$^+$Vβ6$^+$ T cells in the CD4$^+$ T cells of SC in recipient BALB/c WT or NKT KO mice. When DBA/2 SC were injected into untreated BALB/c WT mice on day 0, CD4$^+$Vβ6$^+$ T cells significantly increased to ~35% on day 2 and then eventually declined to the normal range by days 15–21 (Fig. 3*a*). The same result was observed in NKT KO mice. In BALB/c WT mice treated with DBA/2 SC on day 0 and CP on day 2, CD4$^+$Vβ6$^+$ T cells significantly increased to ~35% on day 2, rapidly decreased to the normal range on day 5, and then gradually

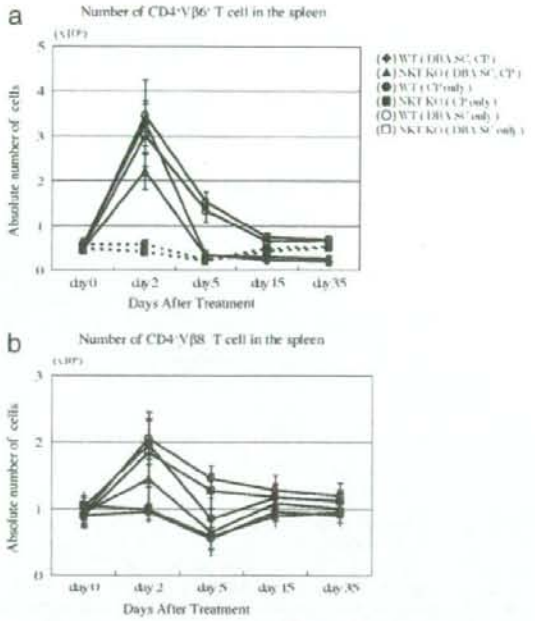

FIGURE 4. Absolute number of cells in the spleen of recipients treated with DBA/2 SC and CP. The kinetics of $CD4^+$ $V\beta6^+$ (*a*) and $CD4^+$ $V\beta8.1/8.2^+$ (*b*) T cells in spleen cells harvested from the recipient BALB/c mice are shown. *a*, The numbers of $CD4^+$ $V\beta6^+$ cells in the spleens from WT mice treated with DBA/2 (DBA) SC and CP (◆; $n = 4$), NKT KO mice treated with DBA/2 SC and CP (▲; $n = 4$), WT mice treated with CP (●; $n = 4$), NKT KO mice treated with CP (■; $n = 4$), WT mice treated with DBA/2 SC (○; $n = 4$), and NKT KO mice treated with DBA/2 SC (□; $n = 4$). *b*, The numbers of $CD4^+V\beta8^+$ cells in the spleens from WT mice treated with DBA/2 SC and CP (◆; $n = 4$), NKT KO mice treated with DBA/2 SC and CP (▲; $n = 4$), WT mice treated with CP (●; $n = 4$), NKT KO mice treated with CP (■; $n = 4$), WT mice treated with DBA/2 SC (○; $n = 4$), and NKT KO mice treated with DBA/2 SC (□; $n = 4$).

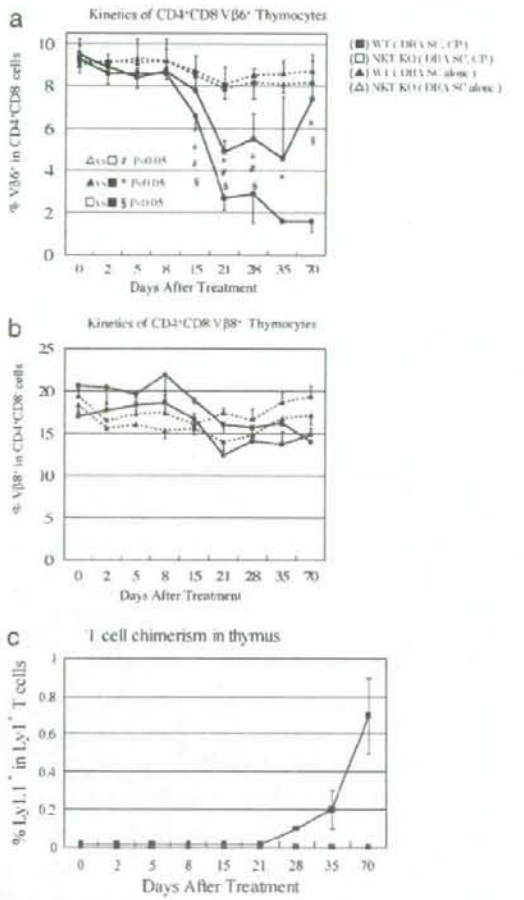

FIGURE 5. Intrathymic clonal deletion in the recipient mice. *a* and *b*, The kinetics of $CD4^+CD8^-V\beta6^+$ (*a*) or $CD4^+CD8^-$ $V\beta8.1/8.2^+$ (*b*) T cells in thymocytes harvested from the recipient BALB/c mice are shown. Thymocytes were labeled with FITC-conjugated anti-Vβ6 or Vβ8.1/8.2 mAb, PE-conjugated anti-CD4 mAb, and allophycocyanin-conjugated anti-CD8 mAb. To determine the percentage of $CD4^+$ T cells that were $V\beta6^+$ or $V\beta8.1/8.2^+$, 10,000–20,000 gated $CD4^+CD8^-$ cells were collected. Thymocytes were obtained from WT mice treated with DBA/2 (DBA) SC and CP (■; $n = 4$), NKT KO mice treated with DBA/2 SC and CP (□; $n = 4$), WT mice treated with DBA/2 SC alone (▲; $n = 4$), and NKT KO mice treated with DBA/2 SC alone (△; $n = 4$). Vertical bars represent SD. The statistical significance of the differences among groups was analyzed and the results are given in *a*. *c*, Intrathymic chimerism in the recipient mice. Thymocytes were labeled with FITC-conjugated anti-Lyt 1.1mAb and PE-conjugated anti-Lyt 1(1.1 + 1.2) mAb. To determine the percentages of T cell chimerism that were $Lyt\ 1.1^+$, 10,000–20,000 gated $Lyt\ 1^+$ cells were collected. Thymocytes were obtained from WT (Lyt-1.2) mice treated with DBA/2 (Lyt-1.1) SC and CP (■; $n = 4$) and NKT KO mice treated with DBA/2 SC and CP (□; $n = 4$). Chimerism was undetectable in WT or NKT KO mice treated with DBA/2 SC alone (data not shown). Vertical bars represent SD.

decreased to ~3%. The percentage of $CD4^+V\beta6^+$ T cells was significantly reduced in BALB/c WT mice treated with DBA/2 SC and CP as compared with that for BALB/c WT mice treated with DBA/2 SC alone. The disappearance of T cells in WBC was specific for $V\beta6^+$ T cells, because the percentage of $V\beta8.1/8.2^+$ T cells was not significantly altered (Fig. 3*b*). Furthermore, the absolute number of $CD4^+V\beta6^+$ T cells in the spleen was analyzed, and similar results were obtained (Fig. 4). We have already reported this phenomenon, which we termed clonal destruction (12, 13), and similar results were obtained in NKT KO mice treated with DBA/2 SC on day 0 and CP on day 2 (Fig. 4). In contrast, when BALB/c WT or NKT KO mice were treated with CP alone on day 2, a transient reduction of both the $CD4^+V\beta6^+$ and $CD4^+V\beta8^+$ T cell subsets was observed.

To further investigate the cellular events in the thymuses of BALB/c mice made tolerant of DBA/2 mice, the association of the clonal deletion with the mixed chimerism was examined (Fig. 5). Whole thymocytes were stained with FITC-conjugated anti-Vβ6 mAb, PE-conjugated anti-CD4 mAb, and allophycocyanin-conjugated anti-CD8 mAb. We previously reported that intrathymic clonal deletion occurs by 6 wk after SC and CP treatment (12, 13), but we did not investigate whether intrathymic CD4 single-positive T cells are depleted by clonal destruction or when intrathymic clonal deletion begins. The present analysis was performed by gating $CD4^+CD8^-$ single-positive thymocytes.

Among the $CD4^+CD8^-$ thymocytes of the BALB/c WT or NKT KO mice, $CD4^+V\beta6^+$ T cells represented ~9% (Fig. 5*a*),

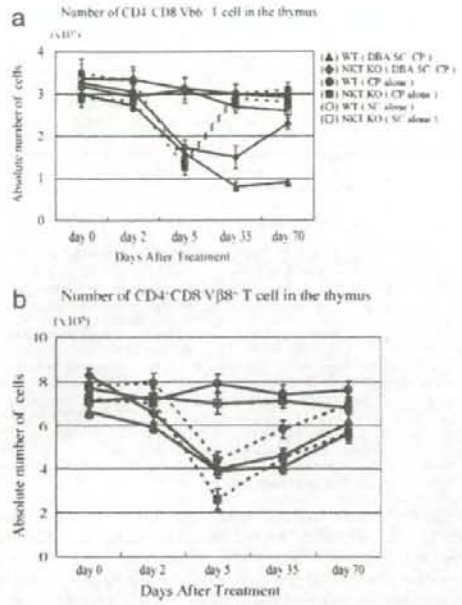

FIGURE 6. Absolute number of cells in the thymuses of recipients treated with DBA/2 (DBA) SC and CP. The kinetics of $CD4^+CD8^-V\beta6^+$ (*a*) and $CD4^+CD8^-$ $V\beta8.1/8.2^+$ (*b*) T cells in thymocytes harvested from the recipient mice are shown. *a*, The numbers of $CD4^+CD8^-V\beta6^+$ cells in the thymuses from WT mice treated with DBA/2 SC and CP (▲; $n = 4$), NKT KO mice treated with DBA/2 SC and CP (◆; $n = 4$), WT mice treated with CP (●; $n = 4$), NKT KO mice treated with and CP (■; $n = 4$), WT mice treated with SC (○; $n = 4$), and NKT KO mice treated with SC (□; $n = 4$). *b*, The numbers of $CD4^+CD8^-V\beta8^+$ cells in the thymuses from WT mice treated with DBA/2 SC and CP (▲; $n = 4$), NKT KO mice treated with DBA/2 SC and CP (◆; $n = 4$), WT mice treated with CP (●; $n = 4$), NKT KO mice treated with CP (■; $n = 4$), WT mice treated with SC (○; $n = 4$), and NKT KO mice treated with SC (□; $n = 4$).

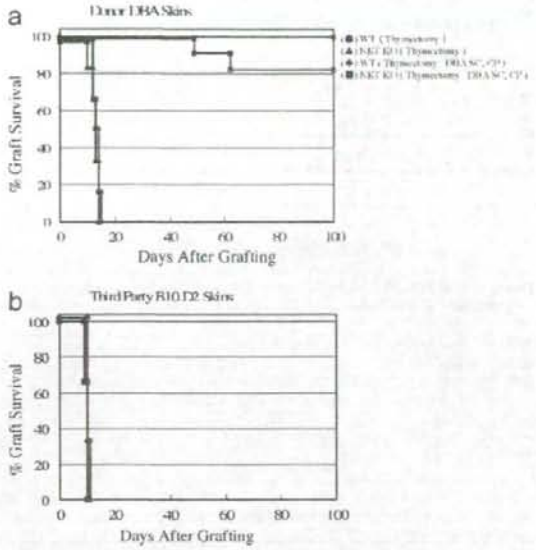

FIGURE 7. Permanent DBA/2 (DBA) skin graft acceptance in the thymectomized BALB/c NKT KO mice treated with DBA/2 SC and CP. Recipient mice were grafted with skin from donor DBA/2 (*a*) or third party B10.D2 (*b*) mice 4 wk after treatment. *a*, The groups and median skin graft survival times were as follows: ●, thymectomized WT mice ($n = 6$; 10 days); ▲, thymectomized NKT KO mice ($n = 6$; 10 days); ◆, thymectomized WT mice treated with DBA/2 SC and CP ($n = 6$; >100 days); ■, thymectomized NKT KO mice treated with DBA/2 SC and CP ($n = 11$; >100 days). *b*, B10.D2 skin grafts were rejected within 14 days after grafting in the following groups: ◆, thymectomized WT mice treated with DBA/2 SC and CP ($n = 3$); and ■, thymectomized NKT KO mice treated with DBA/2 SC and CP ($n = 3$).

and the injection of DBA/2 SC did not significantly alter the percentage of $CD4^+V\beta6^+$ T cells during our observation. In the thymuses of BALB/c WT mice treated with DBA/2 SC and CP, the percentage of $CD4^+V\beta6^+$ T cells was not significantly changed by day 8 but then declined to ~3% by day 21 and reached <2% on day 35. The reduction in $CD4^+V\beta6^+$ T cells was strongly associated with the intrathymic mixed chimerism (Fig. 5*c*). After 28 days, mixed chimerism was detected in the thymuses of BALB/c WT mice treated with DBA/2 SC and CP. In contrast, in the thymuses of NKT KO mice treated with DBA/2 SC and CP, the percentage of $CD4^+V\beta6^+$ T cells was not significantly changed by day 8, then declined to ~5% on day 21, and returned to the normal range by day 70 (Fig. 5*a*). Mixed chimerism was not detected in the thymuses of BALB/c NKT KO mice treated with DBA/2 SC and CP during our observation (Fig. 5*c*). The intrathymic clonal deletion in the tolerant BALB/c mice was specific for Mls-1^a-reactive T cells expressing TCR Vβ6, because $V\beta8.1/8.2^+$ thymocytes were not deleted (Fig. 5*b*). Furthermore, the absolute number of $CD4^-CD8^-V\beta6^+$ thymocytes was analyzed and similar results were obtained (Fig. 6). When BALB/c WT or NKT KO mice were treated with CP alone on day 2, a transient reduction of both $CD4^+V\beta6^+$ and $CD4^+V\beta8^+$ T cell subsets in the thymus was observed.

Induction of skin allograft prolongation in thymectomized NKT KO mice

The previous results indicated that the effector T cells ($CD4^+CD8^-V\beta6^+$) in the thymuses of WT mice were not depleted until intrathymic clonal deletion occurred and that intrathymic clonal deletion was associated with the establishment of mixed chimerism. Thus, we supposed that the effector T cells generated in the thymus at the early phase of tolerance induction were regulated by NKT cells. To confirm this hypothesis, recipients were thymectomized on day −14. As shown in Fig. 7*a*, DBA/2 skin graft survival was permanently prolonged in 9 of 11 recipient NKT KO mice thymectomized on day −14 and treated with SC on day 0 and CP on day 2 (MST, >100 days). Similar results were obtained in thymectomized WT mice ($n = 6$; MST, >100 days). This skin graft prolongation was tolerogen-specific, because third party B10.D2 ($H\text{-}2^d$) allografts were rejected in a normal fashion (Fig. 7*b*).

Generation of tolerogen-specific regulatory T cells in both WT and NKT KO recipients at the late stage of tolerance

Previous studies have demonstrated that the third mechanism of cyclophosphamide-induced tolerance is a regulatory mechanism at the late stage of tolerance (11, 14). To examine whether NKT cells were involved in the generation of regulatory T cells, adoptive transfer experiments were conducted (Fig. 8). BALB/c WT mice were irradiated with 3 Gy and then received an i.v. transfer of 1×10^8 SC from thymectomized WT or NKT KO recipients that had accepted DBA/2 skin grafts for >100 days. With respect to the T

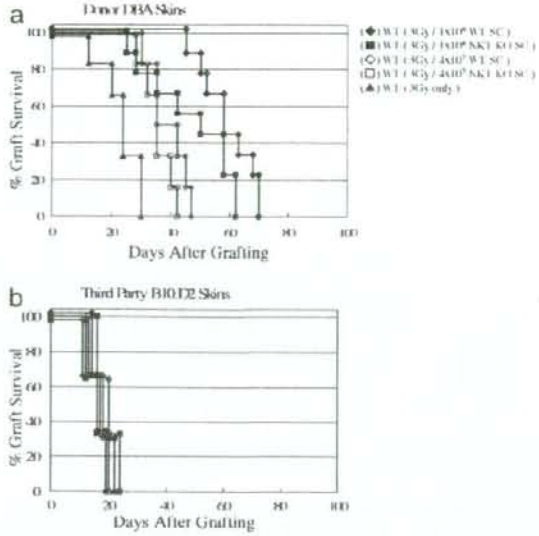

FIGURE 8. Generation of regulatory cells in the recipient mice accepting donor DBA/2 (DBA) skins. BALB/c WT mice were irradiated with 3 Gy and injected i.v. with 1×10^8 or 4×10^7 SC from the thymectomized WT or NKT KO recipients accepting DBA/2 skin grafts >100 days. Recipient mice were grafted with skin from donor DBA/2 (*a*) or third party B10.D2 (*b*) mice 1 day following the transfer of tolerant SC. The groups and median skin graft survival times were as follows: ◆, irradiated WT mice treated with 1×10^8 WT SC (n = 9; 58 days); ■, irradiated WT mice treated with 1×10^8 NKT KO SC (n = 9; 50 days); ◇, irradiated WT mice treated with 4×10^7 WT SC (n = 6; 38.5 days); □, irradiated WT mice treated with 4×10^7 NKT KO SC (n = 6; 35 days); and ▲, irradiated WT mice (n = 6; 24 days). *b*, B10.BR skin grafts were rejected within 24 days after grafting in all groups.

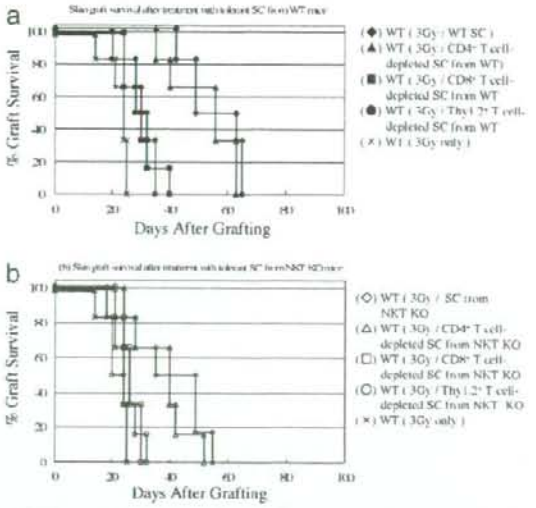

FIGURE 9. Generation of regulatory cells in the recipient mice accepting donor DBA/2 skins. BALB/c WT mice were irradiated with 3 Gy and injected i.v. with 1×10^8 SC from the thymectomized WT or NKT KO recipients accepting DBA/2 skin grafts over 100 days. Recipient mice were grafted with skin from donor DBA/2 mice 1 day following the transfer of tolerant SC. Skin grafting was performed on the same day in all groups. *a*, The groups and median skin graft survival times after treatment with tolerant SC from WT mice were as follows: ◆, irradiated WT mice treated with SC from WT recipients (n = 6; 63 days); ▲, irradiated WT mice treated with CD4+ T cell-depleted SC from WT recipients (n = 6; 56 days); ■, irradiated WT mice treated with CD8+ T cell-depleted SC from WT recipients (n = 6; 29 days); ●, irradiated WT mice treated with Thy1.2+ T cell-depleted SC from WT recipients (n = 6; 32.5 days); and ×, irradiated WT mice (n = 6; 24 days). *b*, The groups and median skin graft survival times after treatment with tolerant SC from NKT KO mice were as follows: ◇, irradiated WT mice treated with SC from NKT KO recipients (n = 6; 42 days); △, irradiated WT mice treated with CD4+ T cell-depleted SC from NKT KO recipients (n = 6; 35 days); □, irradiated WT mice treated with CD8+ T cell-depleted SC from NKT KO recipients (n = 6; 26 days); ○, irradiated WT mice treated with Thy1.2+ T cell-depleted SC from NKT KO recipients (n = 6; 22 days). ×, irradiated WT mice (n = 6; 24 days).

cell percentage of the SC, no significant difference was observed between thymectomized NKT KO mice and BALB/c WT donors (20–25%). Skin grafting was performed 1 day following the transfer of the SC. DBA/2 skin grafts were rejected within 30 days after grafting in the BALB/c WT mice treated with irradiation alone (Fig. 8*a*; n = 6; MST ± SD = 23.3 ± 6.8 days; median = 24 days). The survival of the DBA/2 skin grafts was further prolonged in the irradiated BALB/c WT mice by transferring the SC from thymectomized WT mice that had accepted DBA/2 skin grafts (n = 9; MST ± SD = 59.3 ± 9.1 days; median = 58 days). Similarly, in the irradiated BALB/c WT mice which received the SC transferred from thymectomized NKT KO mice that had accepted DBA/2 skin grafts, the survival of DBA/2 skin grafts was moderately prolonged (n = 9; MST ± SD = 46.7 ± 14.6 days; median = 50 days). There was a statistically significant difference between the graft survivals in irradiated BALB/c WT mice receiving SC transfers from thymectomized WT and NKT KO mice that had accepted DBA/2 skin grafts ($p < 0.05$). In addition, we investigated whether a lower dose of tolerant SC (4×10^7) could induce prolongation of graft survival. Skin graft survival was mildly prolonged in the irradiated BALB/c WT mice by transferring 4×10^7 SC from thymectomized NKT KO mice that had accepted DBA/2 skin grafts (n = 6; MST ± SD = 35.3 ± 5.1 days; median = 35 days). The survival time of the DBA/2 skin grafts was also prolonged in the irradiated BALB/c WT mice by transferring 4×10^7 SC from thymectomized WT mice that had accepted DBA/2 skin grafts (n = 6; MST ± SD = 39.0 ± 6.7 days; median = 38.5 days). In the case of the transfer experiment using low-dose SC, there was no statistically significant difference in survival between the groups treated with 4×10^7 SC from DBA/2 skin graft-accepting thymectomized WT mice and those treated with an equivalent number of SC from DBA/2 skin graft-accepting thymectomized NKT KO mice. The graft survival times in the irradiated BALB/c WT mice treated with a low dose (4×10^7) of SC from DBA/2 skin graft-accepting thymectomized BALB/c WT or NKT KO mice were shorter than those in the irradiated BALB/c WT mice treated with a high dose (1×10^8) of SC. These skin allograft prolongations were tolerogen-specific, because third party skin B10.D2 ($H\text{-}2^d$) allografts were rejected within 24 days after grafting (Fig. 8*b*).

Furthermore, we investigated which T cell subset was dominant in the regulatory function. SC from tolerant BALB/c WT mice were treated with anti-CD4, -CD8, or -Thy-1.2 mAb and complement ex vivo, and 1×10^8 mAb-treated SC were transferred to the irradiated WT mice. Recipient mice were grafted 1 day following the transfer of tolerant SC (Fig. 9*a*). The graft survival time of the recipient treated with CD4+ T cell-depleted SC from tolerant BALB/c WT mice was moderately prolonged (n = 6; MST ±

SD = 52.2 ± 11.9 days; median = 56 days). There was no statistically significant difference compared with the graft survival of the recipient treated with non-T cell-depleted tolerant SC (n = 6; MST ± SD = 55.2 ± 9.7 days; median = 56 days). In contrast, the graft survival of the recipients treated with $CD8^+$ or $Thy1.2^+$ T cell-depleted tolerant SC was significantly shorter than that of the recipients treated with non-T cell-depleted tolerant SC (n = 6; MST ± SD = 29.7 ± 6.0 days; median = 29 days; and n = 6; MST ± SD = 30.0 ± 5.6 days; median = 31 days; respectively). These data indicated that the regulatory cells induced in CP-induced tolerance are mainly $CD8^+$ T cells rather than $CD4^+$ T cells. When SC from tolerant NKT KO mice were used, similar results were obtained (Fig. 9*b*).

Discussion

By using the H-2-matched murine combination of DBA/2 into BALB/c WT and mAbs against T cell markers (Lyt-1.1 and Lyt-1.2) and TCR Vβ6, we have demonstrated the sequential mechanisms of CP-induced tolerance (11, 14). These mechanisms are as follows: 1) clonal destruction of Ag-stimulated and then proliferating T cells by CP at the early stage; 2) intrathymic clonal deletion at the intermediate stage; and 3) regulatory mechanisms at the late stage of tolerance. These three conditions are achieved by SC and 200 mg/kg CP alone without any other supportive treatment in most H-2-matched mouse combinations. In the present study, we have elucidated the roles of NKT cells in the induction of skin allograft tolerance in CP-induced tolerance.

The first mechanism essential to CP-induced tolerance is the selective destruction of Ag-stimulated and then proliferating T cells by CP treatment. This mechanism is considered to be responsible for destroying mature T cells but not immature T cells. As shown in Fig. 3, the $CD4^+V\beta6^+$ T cells that are responsible for the MLR against $Mls\text{-}1^a$-encoded Ag (14) and probably the effector T cells that are responsible for the rejection of DBA/2 skin selectively proliferated on day 2 and were depleted by day 5 in the periphery of the WT mice given DBA/2 SC and CP, leaving most of the nonproliferative $CD4^+V\beta8^+$ T cells. The same results were observed in NKT KO mice given DBA/2 SC and CP, suggesting that NKT-mediated immunoregulation was not required for the induction of clonal destruction in the periphery.

The second mechanism is the intrathymic clonal deletion, which is essential for maintaining the central tolerance in CP-induced tolerance and other chimerism-based tolerance systems (12, 13). By days 28–35 after the treatments with DBA/2 SC and CP, intrathymic chimerism was established due to regeneration of the stem cells of donor origin contained in the tolerogenic SC, and then clonal deletion of $V\beta6^+$ T cells began in the thymuses of WT recipients (Fig. 4). In fact, intrathymic clonal deletion was well correlated with intrathymic mixed chimerism. Notably, in the thymuses of NKT KO recipients given DBA/2 SC and CP, the percentage of $CD4^+V\beta6^+$ T cells decreased only transiently from day 21 through day 35 and returned to the normal level by day 70. Consistently, intrathymic chimerism was not established in NKT KO recipients given DBA/2 SC and CP. Because donor Ag-reactive effector T cells can break mixed chimerism in the periphery, it can be speculated that the effector T cells generated in the thymuses of recipient WT mice by DBA/2 SC administration must be suppressed or regulated by an unsolved mechanism to establish the intrathymic mixed chimerism, which is essential for clonal deletion of donor Ag-specific T cells in the thymus. We hypothesized that this unsolved mechanism could be mediated by the NKT cells. To confirm this hypothesis, we performed a thymectomy and then conditioned the mice with DBA/2 SC and CP (Fig. 7). The results showed that skin graft tolerance was induced in 9 of 11 of the thymectomized NKT KO mice given DBA/2 SC and CP (Fig. 7).

It is important to consider why chimerism or clonal deletion was poorly observed in NKT recipients (group 5; Table I and Fig. 5*a*). Regarding the reduced level of chimerism, we conjectured that chimerism was established by the clonal destruction but was gradually rejected by effector T cells from the thymus. In fact, the level of chimerism was reduced from 2 to 8 wk (group 5; Table I). In BALB/c WT mice, as described above, effector T cells from the thymus were suggested as being regulated by NKT cells, chimerism was stably maintained, and donor skins were permanently accepted. By performing thymectomies in NKT KO mice, a higher level of chimerism could be induced compared with that in non-thymectomized NKT KO mice (group 6 vs 7; Table II). As a result, skin allograft tolerance could be induced in thymectomized NKT KO mice treated with DBA/2 SC and CP. However, the level of chimerism in thymectomized NKT KO mice treated with DBA/2 SC and CP tended to be lower than that in thymectomized BALB/c WT mice treated with DBA/2 SC and CP (group 6 vs group 4; Table II), although this difference did not reach the level of statistical significance. These results may be explained in the following ways. First, we detected T cell chimerism, which may not correlate with bone marrow chimerism. Second, NKT-mediated immunity may contribute to the homeostatic proliferation or self-renewal of T cells. Regarding the poor level of deletion of $CD4^+CD8^-V\beta6^+$ thymocytes in NKT mice (Fig. 5*a*), we can hypothesize that NKT cells may regulate negative selection in the

Table II. *Chimerism and clonal destruction in recipients treated with thymectomy, DBA/2 SC and CP*[a]

						Chimeric Analysis (percent positive cells ± SD)		Analysis of TCR Expression (percent positive cells ± SD)			
		Treatment[a]				Lyt-1.1$^+$/Lyt-1$^+$ (%)		$CD4^+V\beta6^+/CD4^+$ (%)		$CD4^+V\beta6^+/CD4^+$ (%)	
Group	Recipient	Thymectomy (day −14)	SC (day 0)	CP (day 2)	No. of Mice	2 wk	8 wk	3 wk	9 wk	3 wk	9 wk
1	BALB/c WT	(+)	(−)	(−)	6	0		11.7 ± 0.9		18.7 ± 2.1	
2	BALB/c NKT KO	(+)	(−)	(−)	6	0		10.1 ± 1.2		18.9 ± 1.5	
3	DBA/2	(+)	(−)	(−)	6	98.0 ± 2.2		0		13.2 ± 2.0	
4	BALB/c WT	(+)	DBA/2	200[b]	6	3.0 ± 1.0[c]	3.5 ± 1.2[c]	1.1 ± 0.2	0.9 ± 0.7	18.7 ± 0.7	16.9 ± 3.3
5	BALB/c WT	Sham	DBA/2	200[b]	6	2.4 ± 0.9	3.2 ± 1.2	1.7 ± 0.4	1.3 ± 0.5	19.2 ± 1.5	17.4 ± 1.1
6	BALB/c NKT KO	(+)	DBA/2	200[b]	6	2.6 ± 0.5[d]	2.0 ± 0.7[d]	1.3 ± 0.3	1.3 ± 0.2	16.2 ± 0.8	14.7 ± 2.4
7	BALB/c NKT KO	Sham	DBA/2	200[b]	6	1.4 ± 0.3	0.8 ± 0.1	1.5 ± 0.5	1.0 ± 0.4	15.9 ± 1.0	16.7 ± 1.3

[a] The recipient mice were primed i.v. with 1×10^8 viable DBA/2 SC on day 0 and then given 200 mg/kg CP on day 2. Thymectomies were performed on some groups on day −14.
[b] Milligrams per kilogram (mg/kg).
[c] No statistical significance as compared with group 6.
[d] $p < 0.01$ compared with group 7.

thymus. We intend to elucidate these unsolved mechanisms in a future study.

The third mechanism is the generation of regulatory cells in the late stage of tolerance (11, 14). Any significant contribution of suppressor factors, such as enhancing Abs or anti-idiotypic Abs, was excluded from the transfer experiments by using the serum from long-term tolerant mice (11). Recent reports have clarified that the regulatory mechanism is mediated by both $CD25^+CD4^+$ and $CD25^-CD4^+$ T cells via CTLA-4 molecules and Th2 cytokines in mAb-induced tolerance systems (23–25). Furthermore, another study has reported that CP depleted $CD25^+CD4^+$ T cells (26). We have reported that $CD8^+$ T cells are generally involved in the suppressor activity in CP-induced tolerance, whereas $CD4^+$ T cells are not (11, 14). The present study confirmed that $CD8^+$ T cells exhibit the main suppressor activity, indicating that $CD25^+CD4^+$ T cells are not involved in the regulatory mechanisms. One of the aims in the present study was to examine the role of NKT cells in the generation of regulatory cells. The results showed that regulatory cells could be generated without the contribution of NKT cells. However, regarding the suppressor activity, NKT may have some effects on the suppression of the alloreactivity in the recipients, because the survival of DBA/2 skin grafts was significantly longer in irradiated recipients receiving a high dose (1×10^8) of SC from tolerant WT mice than in those receiving the same amount of SC from tolerant NKT KO mice.

Two reports have described the critical role of NKT cells in inducing transplantation tolerance (5, 6). However, the precise mechanisms at the cellular and molecular levels have remained unclear. It has been well documented that NKT cells produce large amounts of both IL-4 and IFN-γ upon activation (27–29). Given that IL-4 and IFN-γ have opposite effects on the development of Th1 and Th2 cells, extensive analyses have been performed with various experimental systems, and conflicting results have been reported (30–32). By using IL-4 KO and IFN-γ KO mice, two groups analyzed the mechanisms of the NKT-mediated role in transplantation tolerance induction and produced conflicting results (5, 6). Ikehara et al. (6) suggested that there was little involvement of these two cytokines in C57BL/6 mice injected with anti-CD4 mAb and grafted with rat islets. In contrast, Seino et al. (5) suggested that IFN-γ partially contributes to tolerance induction in C57BL/6 mice injected with anti-LFA-1 and ICAM-1 mAbs and grafted with heart grafts from BALB/c ($H\text{-}2^d$) mice. However, these results did not seem to be definitive, because they could not show clearly whether the IFN-γ produced by NKT cells was involved in one or more of the steps that induce and maintain transplantation tolerance, i.e., activation of effector T cells, apoptosis of effector T cells, reprogramming of effector T cells (anergy induction), and the generation of regulatory T cells. In the present study, we can strongly suggest two roles for NKT cells in CP-induced tolerance. One is to regulate the effector T cells generated in the thymuses of recipient WT mice by DBA/2 SC administration through the establishment of intrathymic clonal deletion. The other is to allow generation of regulatory cells without NKT cell-mediated immunoregulation.

As for the NKT reconstitution assay (Fig. 2), unfortunately we could not show how many NKT cells are needed to completely reconstitute NKT-mediated immunoregulation. In our laboratory, the Vα14 transgenic mice (RAG-1 KO background) needed for reconstituting NKT cells in NKT (Vα14) KO mice are unavailable. However, even in the experiments using the Vα14 transgenic mice, a previous attempt to perform adoptive transfer of $V\alpha14^+$ cells from Vα14 transgenic mice in an allogeneic tolerance system was not successful, probably because the dose of $V\alpha14^+$ cells was not sufficient to restore these cells to the normal level (Y. Yasunami, unpublished observation). We initially transferred 1×10^8 SC from WT mice to NKT KO mice but could not induce permanent acceptance donor skin grafts in three of seven recipients. NKT (αGalCer/CD1d tetramer$^+$CD3$^+$) cells were restored to 0.4 and 4.3% in SC and LMNC of these mice, respectively, suggesting that the level of NKT reconstitution was not enough. In contrast, Seino et al. had reconstituted WT BMC (including NKT cells and progenitors) in irradiated NKT KO mice (5). To further reconstitute NKT cells, recipient NKT KO mice were irradiated with 3 Gy and reconstituted with SC and BMC from WT mice. Although NKT cells were not fully restored (0.7 and 9.5% in SC and LMNC, respectively), permanent skin graft acceptance was induced in all of the irradiated and reconstituted NKT KO mice.

Acknowledgments

We thank Dr. Hisanori Mayumi, General Manager, Watanabe Hospital (Kagoshima, Japan) for reviewing this manuscript and giving helpful comments. We also thank the Edanz Editing Co. Ltd. (Fukuoka, Japan) and KN International, Inc. (Iowa City, IA) for the English editing of this manuscript.

Disclosures

The authors have no financial conflict of interest.

References

1. Cui, J., T. Shin, T. Kawano, H. Sato, E. Kondo, I. Toura, Y. Kaneko, H. Koseki, M. Kanno, and M. Taniguchi. 1997. Requirement for Vα14 NKT cells in IL-12-mediated rejection of tumors. *Science* 278: 1623–1626.
2. Mieza, M. A., T. Itoh, J. Q. Cui, Y. Makino, T. Kawano, K. Tsuchida, T. Koike, T. Shirai, H. Yagita, A. Matsuzawa, et al. 1996. Selective reduction of $V\alpha14^+$ NK T cells associated with disease development in autoimmune-prone mice. *J. Immunol.* 156: 4035–4040.
3. Slifka, M. K., R. R. Pagarigan, and J. L. Whitton. 2000. NK markers are expressed on a high percentage of virus-specific $CD8^+$ and $CD4^+$ T cells. *J. Immunol.* 164: 2009–2015.
4. Naiki, Y., H. Nishimura, T. Kawano, Y. Tanaka, S. Itohara, M. Taniguchi, and Y. Yoshikai. 1999. Regulatory role of peritoneal $NK1.1^+$ $\alpha\beta$ T cells in IL-12 production during *Salmonella* infection. *J. Immunol.* 163: 2057–2063.
5. Seino, K. I., K. Fukao, K. Muramoto, K. Yanagisawa, Y. Takada, S. Kakuta, Y. Iwakura, L. Van Kaer, K. Takeda, T. Nakayama, et al. 2001. Requirement for natural killer T (NKT) cells in the induction of allograft tolerance. *Proc. Natl. Acad. Sci. USA* 98: 2577–2581.
6. Ikehara, Y., Y. Yasunami, S. Kodama, T. Maki, M. Nakano, T. Nakayama, M. Taniguchi, and S. Ikeda. 2000. $CD4^+$ Vα14 natural killer T cells are essential for acceptance of rat islet xenografts in mice. *J. Clin. Invest.* 105: 1761–1767.
7. Shin, T., H. Mayumi, K. Himeno, H. Sanui, and K. Nomoto. 1984. Drug-induced tolerance to allografts in mice. I. Difference between tumor and skin grafts. *Transplantation* 37: 580–584.
8. Mayumi, H., T. Shin, K. Himeno, and K. Nomoto. 1985. Drug-induced tolerance to allografts in mice II. Tolerance to tumor allografts of large doses associated with rejection of skin allografts and tumor allografts of small doses. *Immunobiology* 169: 147–161.
9. Mayumi, H., K. Himeno, T. Shin, and K. Nomoto. 1985. Drug-induced tolerance to allografts in mice. IV. Mechanisms and kinetics of cyclophosphamide-induced tolerance. *Transplantation* 39: 209–215.
10. Mayumi, H., K. Himeno, K. Tanaka, N. Tokuda, J. L. Fan, and K. Nomoto. 1986. Drug-induced tolerance to allografts in mice. IX. Establishment of complete chimerism by allogeneic spleen cell transplantation from donors made tolerant to H-2-identical recipients. *Transplantation* 42: 417–422.
11. Tomita, Y., H. Mayumi, M. Eto, and K. Nomoto. 1990. Importance of suppressor T cells in cyclophosphamide-induced tolerance to the non-H-2-encoded alloantigens. Is mixed chimerism really required in maintaining a skin allograft tolerance? *J. Immunol.* 144: 463–473.
12. Eto, M., H. Mayumi, Y. Tomita, Y. Yoshikai, and K. Nomoto. 1990. Intrathymic clonal deletion of $V\beta6^+$ T cells in cyclophosphamide-induced tolerance to H-2-compatible, Mls-disparate antigens. *J. Exp. Med.* 171: 97–113.
13. Tomita, Y., Y. Nishimura, N. Harada, M. Eto, K. Ayukawa, Y. Yoshikai, and K. Nomoto. 1990. Evidence for involvement of clonal anergy in MHC class I and class II disparate skin allograft tolerance after the termination of intrathymic clonal deletion. *J. Immunol.* 145: 4026–4036.
14. Eto, M., H. Mayumi, Y. Tomita, Y. Yoshikai, Y. Nishimura, and K. Nomoto. 1990. Sequential mechanisms of cyclophosphamide-induced skin allograft tolerance including the intrathymic clonal deletion followed by late breakdown of the clonal deletion. *J. Immunol.* 145: 1303–1310.
15. Zhang, Q. W., H. Mayumi, M. Umesue, Y. Tomita, K. Nomoto, and H. Yasui. 1997. Fractionated dosing of cyclophosphamide for establishing long-lasting skin allograft survival, stable mixed chimerism, and intrathymic clonal deletion in mice primed with allogeneic spleen cells. *Transplantation.* 63: 1667–1673.
16. Maeda, T., M. Eto, Y. Nishimura, K. Nomoto, and Y. Y. Kong. 1993. Role of peripheral hemopoietic chimerism in achieving donor-specific tolerance in adult mice. *J. Immunol.* 150: 753–762.

17. Yoshikawa, M., Y. Tomita, T. Uchida, Q. W. Zhang, and K. Nomoto. 1999. Lack of pluripotent stem cell engraftment in cyclophosphamide-induced tolerance. *Transplant. Proc.* 31: 898–899.
18. Yoshikawa, M., Y. Tomita, T. Uchida, Q. W. Zhang, I. Shimizu, and K. Nomoto. 1999. Cyclophosphamide 200 mg/kg lacks ability to induce pluripotent stem cell engraftment in mice. *Transplant. Proc.* 31: 1939.
19. Tomita, Y., M. Yoshikawa, Q. W. Zhang, I. Shimizu, S. Okano, T. Iwai, H. Yasui, and K. Nomoto. 2000. Induction of permanent mixed chimerism and skin allograft tolerance across fully MHC-mismatched barriers by the additional myelosuppressive treatments in mice primed with allogeneic spleen cells followed by cyclophosphamide. *J. Immunol.* 165: 34–41.
20. Mayumi, H., K. Nomoto, and R. A. Good. 1988. A surgical technique for experimental free skin grafting in mice. *Jpn. J. Surg.* 18: 548–557.
21. Tomita, Y., A. Khan, and M. Sykes. 1994. Role of intrathymic clonal deletion and peripheral anergy in transplantation tolerance induced by bone marrow transplantation in mice conditioned with a nonmyeloablative regimen. *J. Immunol.* 153: 1087–1098.
22. Matsuda, J. L., O. V. Naidenko, L. Gapin, T. Nakayama, M. Taniguchi, C. R. Wang, Y. Koezuka, and M. Kronenberg. 2000. Tracking the response of natural killer T cells to a glycolipid antigen using CD1d tetramers. *J. Exp. Med.* 192: 741–754.
23. Graca, L., S. Thompson, C. Y. Lin, E. Adams, S. P. Cobbold, and H. Waldmann. 2002. Both $CD4^+CD25^+$ and $CD4^+CD25^-$ regulatory cells mediate dominant transplantation tolerance. *J. Immunol.* 168: 5558–5565.
24. Taylor, P. A., R. J. Noelle, and B. R. Blazar. 2001. $CD4^+CD25^+$ immune regulatory cells are required for induction of tolerance to alloantigen via costimulatory blockade. *J. Exp. Med.* 193: 1311–1318.
25. Kingsley, C. I., M. Karim, A. R. Bushell, and K. J. Wood. 2002. $CD25^+CD4^+$ regulatory T cells prevent graft rejection: CTLA-4- and IL-10-dependent immunoregulation of alloresponses. *J. Immunol.* 168: 1080–1086.
26. Ghiringhelli, F., N. Larmonier, E. Schmitt, A. Parcellier, D. Cathelin, C. Garrido, B. Chauffert, E. Solary, B. Bonnotte, and F. Martin. 2004. $CD4^+CD25^+$ regulatory T cells suppress tumor immunity but are sensitive to cyclophosphamide which allows immunotherapy of established tumors to be curative. *Eur. J. Immunol.* 34: 336–344.
27. Arase, H., N. Arase, K. Ogasawara, R. A. Good, and K. Onoe. 1992. An $NK1.1^+$ $CD4^+8^-$ single-positive thymocyte subpopulation that expresses a highly skewed T-cell antigen receptor Vβ family. *Proc. Natl. Acad. Sci. USA* 89: 6506–6510.
28. Kawano, T., J. Cui, Y. Koezuka, I. Toura, Y. Kaneko, K. Motoki, H. Ueno, R. Nakagawa, H. Sato, E. Kondo, et al. 1997. CD1d-restricted and TCR-mediated activation of Vα14 NKT cells by glycosylceramides. *Science* 278: 1626–1629.
29. Yoshimoto, T., and W. E. Paul. 1994. CD4pos, NK1.1pos T cells promptly produce interleukin 4 in response to in vivo challenge with anti-CD3. *J. Exp. Med.* 179: 1285–1295.
30. Cui, J., N. Watanabe, T. Kawano, M. Yamashita, T. Kamata, C. Shimizu, M. Kimura, E. Shimizu, J. Koike, H. Koseki, et al. 1999. Inhibition of T helper cell type 2 cell differentiation and immunoglobulin E response by ligand-activated Vα14 natural killer T cells. *J. Exp. Med.* 190: 783–792.
31. Burdin, N., L. Brossay, and M. Kronenberg. 1999. Immunization with α-galactosylceramide polarizes CD1-reactive NK T cells towards Th2 cytokine synthesis. *Eur. J. Immunol.* 29: 2014–2025.
32. Singh, N., S. Hong, D. C. Scherer, I. Serizawa, N. Burdin, M. Kronenberg, Y. Koezuka, and L. Van Kaer. 1999. Cutting edge: activation of NK T cells by CD1d and α-galactosylceramide directs conventional T cells to the acquisition of a Th2 phenotype. *J. Immunol.* 163: 2373–2377.

The EMBO Journal (2007) 26, 113–122 | © 2007 European Molecular Biology Organization | All Rights Reserved 0261-4189/07
www.embojournal.org

THE EMBO JOURNAL

Cytoplasmic destruction of p53 by the endoplasmic reticulum-resident ubiquitin ligase 'Synoviolin'

Satoshi Yamasaki[1,14], Naoko Yagishita[1,14], Takeshi Sasaki[1,14], Minako Nakazawa[1,14], Yukihiro Kato[1,14], Tadayuki Yamadera[1,14], Eunkyung Bae[2,14], Sayumi Toriyama[1], Rie Ikeda[1], Lei Zhang[1], Kazuko Fujitani[1], Eunkyung Yoo[2], Kaneyuki Tsuchimochi[1], Tomohiko Ohta[3], Natsumi Araya[1], Hidetoshi Fujita[1], Satoko Aratani[1], Katsumi Eguchi[4], Setsuro Komiya[5], Ikuro Maruyama[6], Nobuyo Higashi[7], Mitsuru Sato[7], Haruki Senoo[7], Takahiro Ochi[8], Shigeyuki Yokoyama[9], Tetsuya Amano[1], Jaeseob Kim[2], Steffen Gay[10], Akiyoshi Fukamizu[11], Kusuki Nishioka[12], Keiji Tanaka[13] and Toshihiro Nakajima[1,*]

[1]Department of Genome Science, Institute of Medical Science, St Marianna University School of Medicine, Kawasaki, Japan, [2]GenExl, Inc. Biomedical Research Center, Taejon, South Korea, [3]Division of Breast and Endocrine Surgery, Institute of Medical Science, St Marianna University School of Medicine, Kawasaki, Japan, [4]The First Department of Internal Medicine, Nagasaki University School of Medicine, Nagasaki, Japan, [5]Department of Orthopedic Surgery, Kagoshima University, Faculty of Medicine, Kagoshima, Japan, [6]Department of Dermatology and Laboratory of Molecular Medicine, Kagoshima University, Faculty of Medicine, Kagoshima, Japan, [7]Department of Anatomy, Akita University School of Medicine, Akita, Japan, [8]National Hospital Organization Sagamihara National Hospital, Kanagawa, Japan, [9]Department of Biophysics and Biochemistry, Graduate School of Science, University of Tokyo, Tokyo, Japan; Protein Research Group, RIKEN Genomic Sciences Center, Yokohama, Japan, [10]Department of Rheumatology, University Hospital Zürich, Zürich, Switzerland, [11]Aspect of Functional Genomic Biology, Center of Tsukuba Advanced Research Alliance, University of Tsukuba, Tsukuba, Japan, [12]Rheumatology, Immunology and Genetics Program, Institute of Medical Science, St Marianna University School of Medicine, Kawasaki, Japan and [13]Laboratory of Frontier Science, The Tokyo Metropolitan Institute of Medical Science, Tokyo, Japan

Synoviolin, also called HRD1, is an E3 ubiquitin ligase and is implicated in endoplasmic reticulum -associated degradation. In mammals, Synoviolin plays crucial roles in various physiological and pathological processes, including embryogenesis and the pathogenesis of arthropathy. However, little is known about the molecular mechanisms of Synoviolin in these actions. To clarify these issues, we analyzed the profile of protein expression in *synoviolin*-null cells. Here, we report that Synoviolin targets tumor suppressor gene p53 for ubiquitination. Synoviolin sequestrated and metabolized p53 in the cytoplasm and negatively regulated its cellular level and biological functions, including transcription, cell cycle regulation and apoptosis. Furthermore, these p53 regulatory functions of Synoviolin were irrelevant to other E3 ubiquitin ligases for p53, such as MDM2, Pirh2 and Cop1, which form autoregulatory feedback loops. Our results provide novel insights into p53 signaling mediated by Synoviolin.

The EMBO Journal (2007) **26**, 113–122. doi:10.1038/sj.emboj.7601490; Published online 14 December 2006
Subject Categories: proteins
Keywords: apoptosis; cell growth; E3 ubiquitin ligase; endoplasmic reticulum-associated degradation; rheumatoid arthritis

Introduction

The ubiquitin–proteasome system (UPS) consists of a small polypeptide ubiquitin, a framework of enzymes that mediates the covalent attachment of ubiquitin to proteolytic substrates and the 26S proteasome that digests the modified proteins into peptides. The formation of ubiquitin conjugates requires the successive action of three classes of enzymes. This process is first activated by an E1 (activating enzyme) in an ATP-dependent manner, forming a high-energy thioester bond between ubiquitin and an E1, and the activated ubiquitin is then transferred to an E2 (conjugating enzyme), forming a similar thioester linkage between ubiquitin and E2, and then E3 ubiquitin ligase transfers ubiquitin to the target proteins. Through repeated reactions of this cycle, a polyubiquitin chain is formed on the target proteins, which is recognized by the 26S proteasome for ultimate degradation (Hershko and Ciechanover, 1998; Pickart, 2001). In the UPS pathway, the E3 ubiquitin ligases play critical roles in the selection of target proteins for degradation, because each distinct E3 ubiquitin ligase usually binds a protein substrate with a degree of selectivity for ubiquitination in a temporally and spatially regulated fashion.

Synoviolin, a representative of endoplasmic reticulum (ER)-resident E3 ubiquitin ligases, is a mammalian homolog of Hrd1p/Der3p that "substrates" misfolded carboxypeptide yscY (CPY*) (Bordallo *et al*, 1998) and 3-hydroxy-3-methylglutaryl-coenzyme A reductase (HMGR), a key enzyme of the mevalonate pathway in yeast (Shearer and Hampton, 2004, 2005). We cloned Synoviolin from rheumatoid synovial cells (RSCs) and described that Synoviolin is highly expressed in synoviocytes of patients with rheumatoid arthritis (RA) (Amano *et al*, 2003). In that report, we demonstrated that overexpression of Synoviolin in transgenic mice leads to advanced arthropathy caused by reduced apoptosis of synoviocytes. On the other hand, *synoviolin*$^{+/-}$ mice showed resistance to the development of arthritis owing to enhanced

*Corresponding author. Department of Genome Science, Institute of Medical Science, St Marianna University School of Medicine, 2-16-1 Sugao Miyamae-ku, Kawasaki, Kanagawa 216-8512, Japan. Tel.: +81 44 977 8111 (ext. 4111); Fax: +81 44 977 10712; E-mail: nakashit@marianna-u.ac.jp
[14]These authors contributed equally to this work

Received: 11 April 2006; accepted: 7 November 2006; published online: 14 December 2006